SURFACE ROUGHNESS EFFECTS ON NUCLEATE BOILING HEAT TRANSFER RATES

JAMES C. GIBSON, JR.

SURFACE ROUGHNESS EFFECTS ON NUCLEATE BOILING HEAT TRANSFER RATES

by

James C. Gibson, Jr
Lieutenant, United States Navy

Submitted in partial fulfillment of

the requirements for the degree of

MASTER OF SCIENCE
IN
MECHANICAL ENGINEERING

United States Naval Postgraduate School
Monterey, California

1 9 6 2

SURFACE ROUGHNESS EFFECTS ON NUCLEATE BOILING HEAT TRANSFER RATES

* * * * *

James C. Gibson, Jr.

UNITED STATES NAVAL POSTGRADUATE SCHOOL

Degree: Master of Science in Mechanical Engineering

Classification:

Thesis: Unclassified

Abstract: Unclassified

Title of Thesis: Unclassified

Contains no proprietary information

SURFACE ROUGHNESS EFFECTS ON

NUCLEATE BOILING HEAT TRANSFER RATES

by

James C. Gibson, Jr.

This work is accepted as fulfilling

the thesis requirements for the degree of

MASTER OF SCIENCE

IN

MECHANICAL ENGINEERING

from the

United States Naval Postgraduate School

ABSTRACT

Heat transfer rates were measured for pool boiling, in the nucleate regime at one atmosphere pressure, for distilled water on a horizontal, flat, stainless steel (Type 304) plate.

The heating surfaces were prepared with different degrees of roughness by common machining operations. Heat was supplied to the specimen by a nichrome wire heating coil mounted in a Lavite block which supported the specimen.

Results are presented as Δt_m, temperature difference between the heating surface and the distilled water, as a function of heat rate, q/A for a given surface roughness.

Heat rates covered a range from a maximum of 29,000 Btu/hr ft^2 to a minimum of 2550 Btu/hr ft^2 while Δt_m varied from 39° to 0.5°F. Ten surface roughnesses were tested in the range of 3 to 100 micro inches rms. One specimen with .005 in. grooves and another with .008 in. grooves were also tested.

The results indicate that as surface roughness increased the Δt_m necessary to maintain a given heat rate decreased until a roughness of about 30 μin. rms. Thereafter, little effect of increased roughness was noted. As an example for a heat rate, q/A, of 20,000 Btu/hr ft^2, Δt_m was 36.5°F for a roughness of 3.1 μin rms. and decreased to 17.5 °F at 23 μin rms.

TABLE OF CONTENTS

ITEM	TITLE	PAGE
	Abstract	ii
	Table of Symbols	iv
	List of Figures	v
	Acknowledgment	vii
Chapter I	Introduction	1
Chapter II	Description of Equipment	5
Chapter III	Experimental Procedures and Surface Roughness Measurement	11
Chapter IV	Discussion of Results and Conclusions	13
Bibliography		19
Appendix A	Graphical and Tabular Results	21
Appendix B	Sample Calculations, Tables, Drawings, and Photographs	49

TABLE OF SYMBOLS

A	Exposed, horizontal, projected area of test specimen, sq. in.
h	Surface heat transfer coefficient, Btu/hr ft^2 °F
k	Thermal conductivity, Btu/hr ft °F
q	Heat transferred per unit time, Btu/hr
Δt_m	Temperature difference between surface of the test specimen and bulk temperature of water, °F
V	Voltage drop across specimen heating coil, volts
I	Current through specimen heating coil, amps
t	Temperature, °F

LIST OF FIGURES AND TABLES

FIGURE	TITLE	PAGE
1	Typical Boiling Curve	54
2	Overall Equipment Layout	55
3	Circular Test-Specimen and Thermocouple Placement	56
4	Test Specimen (circular)	57
5	Mounting Block-Plan View	58
6	Mounting Block Elevation View	59
7	Mounting Block	60
8	Mounting Block in Water Bath	61
9	Rectangular Test-Specimen and Thermocouple Placement	62
10	Test Specimen (rectangular)	63
11	Thermocouple Circuit Diagram	64
12	Heating Coil (rectangular)	65
13	Heating Coil (circular)	66
14	Electrical Circuit Diagram	67
15	Surface Analyzer Equipment	68
16	Location of Surface Roughness Measurements	69
17	Plot of Heat Rate vs. Δt_m, rectangular specimens #1-10, (all roughnesses)	25
18	Plot of Heat Rate vs. Δt_m, rectangular and circular specimens #9 (5.3 μ in).	26
19	Plot of Heat Rate vs. Δt_m, rectangular and circular specimens #6 (23 μin)	27
20	Plot of Heat Rate vs. Δt_m, rectangular specimen specimen #7 (15 μin)	28
21	Plot of Heat Rate vs. Δt_m, rectangular specimen #8 (7.4 μin)	29
22	Plot of Heat Rate vs. Δt_m, rectangular specimens #1 & 2 (macro roughness)	30

FIGURE	TITLE	PAGE
23	Plot of Heat Rate vs. Δt_m, rectangular specimen #1 (.008 in)	31
24	Plot of Heat Rate vs. Δt_m, rectangular specimen #2 (.005 in)	32
25	Plot of Heat Rate vs. Δt_m, rectangular specimen #3 (96 μin)	33
26	Plot of Heat Rate vs. Δt_m, rectangular specimen #4 (46 μin)	34
27	Plot of Heat Rate vs. Δt_m, rectangular specimen #5 (32 μin)	35
28	Plot of Heat Rate vs. Δt_m, rectangular specimen #6 (23 μin)	36
29	Plot of Heat Rate vs. Δt_m, rectangular specimen #7 (15 μin)	37
30	Plot of Heat Rate vs. Δt_m, rectangular specimen #8 (7.4 μin)	38
31	Plot of Heat Rate vs. Δt_m, rectangular specimen #9 (5.3 μin)	39
32	Plot of Heat Rate vs. Δt_m, rectangular specimen #10 (3.1 μin)	40
33	Plot of Heat Rate vs. Δt_m, circular specimen #6 (23 μin)	41
34	Plot of Heat Rate vs. Δt_m, circular specimen #9 (5.3 μin)	42
35	Plot of Heat Rate vs. Δt_m, rectangular specimen #8 (7.4 μin)	43
36	Plot of Heat Rate vs. Δt_m, rectangular specimen #7 (15 μin)	44
37	Plot of Roughness vs. Δt_m, for various heat rates	45
38	Plot of Heat Rate vs. Δt_m, rectangular specimens #1-10 (all roughnesses)	46
39	Plot of Surface Coefficient vs. Δt_m, rectangular specimens #1-10 (all roughnesses)	47
40	Plot of Roughness vs. Δt_m for surface coefficient h = 1000 Btu/hr ft^2 °F	48
TABLE I	Specimen Identification	70
TABLE II	Sample Data Sheet	71
TABLE III	Experimental Results	22

ACKNOWLEDGMENT

The preliminary investigation of this topic was carried out during a six-week field trip at the U. S. Naval Boiler and Turbine Laboratory in Philadelphia. The writer wishes to thank CDR H. S. Morton, USN, and his able staff for their time and effort spent in helping to accumulate background information in the nucleate boiling field.

The writer desires to express his appreciation to Professor P. F. Pucci, who acted as thesis advisor. Without his help and continued guidance, the completion of this thesis would not have been possible.

CHAPTER I

INTRODUCTION

Developments in nuclear reactors and rocket engines, where exceedingly high heat quantities are transferred in comparatively small areas, have focused attention on boiling as a mode of transferring heat at high flux densities.

There exist three types of boiling, namely, nucleate, transition, and film boiling. [5] [1] The change from one type to another is accompanied by marked differences in the thermal states of the system. A typical boiling curve is shown in Figure 1. Nucleate boiling starts when the temperature of the surface exceeds the saturation temperature by a few degrees. Next to the solid surface a thin layer of superheated liquid is formed in which bubbles nucleate and grow from some preferred spots. In nucleate boiling a temperature increase is accompanied by a sharp increase of the heat flux and of the bubble population. The spots where bubbles originate become more numerous until a critical temperature is reached at which a maximum heat flux is attained. At that point the bubbles are so numerous that they interfere with each other. If the temperature is increased beyond the critical value by a few degrees the transition boiling begins. The surface is blanketed by an unstable, irregular film of vapor which is in violent motion. A further increase of the temperature of the surface is followed by a decrease of the heat flux until a minimum value is reached at which a stable film of vapor is formed between the heating surface and liquid. The

1 Numbers in brackets refer to references listed in the Bibliography

stable film boiling is characterized by an orderly discharge of large bubbles with a regular frequency and at regular intervals. In the film-boiling region, the heat flux increases with an increase of temperature, but at a much slower rate than in nucleate boiling. Consequently, as the heat-transfer rate is increased in this region, the temperature of the heating surface rises rapidly and can exceed the melting point of the heating surface causing failure.

It has been generally agreed [1, 4, 8, 10, 15] that the high heat transfer rates associated with the nucleate boiling region are due primarily to agitation created by the motion of the bubbles in the superheated liquid adjacent to the heated surface. The rate therefore depends upon:

(1) the size at which a bubble will detach itself

(2) the rate at which a bubble forms

(3) the speed of rise of the bubble

(4) the number of bubbles generated

Since heat transfer rate is a function of bubble formation, knowledge of the factors affecting the behavior of these bubbles is essential to understanding the nucleate boiling problem.

From a photographic study Jakob [11] discovered that the product of bubble diameter when breaking off from the heated surface and the frequency of bubble formation seemed to be constant.

Perkins and Westwater [9] found that for nucleate boiling of methanol at heat fluxes up to 80% of the maximum, not only was the product of bubble diameter and frequency constant but also both factors were constant themselves for a given heat flux. From this they concluded that the increase in heat flux with increase in Δt, difference between the temperature of the

heated surface and that of the boiling liquid, must be caused entirely by a corresponding increase in the number of nucleating sites on the heating surface.

Gaertner and Westwater [14] determined the number of active sites in the nucleate region for a boiling liquid on a horizontal, flat, copper surface by plating a thin layer of nickel on the copper surface and counting the number of pinholes in the plate after a boiling run. They found that a linear relationship between the number of active sites and the heat flux as suggested by Jakob [11] and Corty and Foust [4] did not hold for their system but that heat flux was proportional approximately to the square root of the number of sites.

Griffith and Wallis [3] proposed that nucleation occurs from pre-existing gas filled cavities on the surface and that a single dimension, size distribution of the cavities, is sufficient to fix the nucleation characteristics of that surface. Therefore the wall superheat should be directly related to the size of the cavity for a particular liquid-surface combination and heat input.

Cavities exist in the metallic surface and in these cavities vapor is trapped after an earlier bubble has broken loose. The trapped vapor then acts as the nucleus for the next bubble from the same spot. A vapor filled cavity may act as a nucleus for the bubble formation as long as the superheat in the surface is high enough to support the vapor phase inside the cavity.

It is apparent from the above investigations that the heat flux is a function of the active centers. Active centers are agreed to be the valleys of a groove of a certain size which generate bubbles of constant size regardless of the heat flux or Δ -, when bubbles have once started to

form from that spot. Therefore the number of nuclei of a certain size may be expected to be proportional to the number of grooves of corresponding size.

Because of this apparent relation between number of active sites, heat flux and number and size of grooves, several experimenters [1, 2, 3, 4, 15] have investigated the effects of surface roughness on nucleate boiling heat transfer rates. They have found that for a given heat transfer rate the Δt necessary to maintain nucleate boiling decreases with increasing roughness. Corty and Foust [4] in their work with N-pentane and nickel indicate that this is true up to a roughness of about 25-30 micro inches rms and that for rougher surfaces the Δt necessary for nucleate boiling remains constant.

The purposes of this investigation were two fold:

(1) To study the effect of surface roughness on heat transfer rates for pool boiling in the nucleate regime from a horizontal, flat plate for one of the most common surface-liquid combinations in use today, stainless steel and distilled water. Specimens with roughnesses corresponding to those previously investigated were studied as well as several with much rougher surfaces.

(2) Previous investigators have dealt with specially prepared surfaces. The second purpose of this study was to see if surfaces roughened by common machining operations such as shaping, milling, grinding and polishing show the same trends as the laboratory prepared specimens. The roughnesses of these surfaces were determined by use of a Brush Surface Analyzer.

CHAPTER II

DESCRIPTION OF EQUIPMENT

1. General Description.

The equipment consists of the following components:

A. Test specimens providing the heat transfer surface

B. Mounting block for test specimens

C. Temperature sensing and indicating devices

D. Power supply and power measurement equipment

E. Surface roughness equipment

The arrangement of the equipment is shown in the photograph, Figure 2.

2. Detailed Descriptions.

A. Test Specimens.

The test specimens were Type 304, stainless steel plates, 2-1/2 inches by 4 inches, 1/2 inch thick. Each specimen was prepared by various machining operations to obtain the desired surface finish. The specimens are numbered 1 through 10 in order of decreasing roughness; the identification number together with surface finish, and preparatory machining are listed in Table I.

Specimens of this size were chosen because it was felt that they would be large enough to minimize end effects and small enough to obtain a fairly uniform finish over the entire heat transferring surface. This size was also suitable for specimen instrumentation.

Each specimen was fitted with six thermocouples for determining

the temperature of the finished surface. Thermocouple design and placement is described in paragraph C of this chapter. All specimens were first finished on a shaper with minimum tool advance. This operation produced the finish desired for specimen #5. The specimens to have finer finishes were then further prepared as listed in Table I. To roughen specimens #3 and #4 from the base finish, they were cut on a milling machine with slow feed. Specimen #2 was roughened by making a 0.005 inch cut with one pass of the milling machine running at 1-3/8 ipm. After testing, specimen #2 was further roughened by making a 0.008 inch cut, perpendicular to the original mill cut, on a shaper with a .050" cross feed advance. This was used as specimen #1.

In addition to the rectangular specimens, two circular ones were tested. After testing specimens #6 and #9 they were machined on a lathe to a 2-1/2 inch diameter circular shape. By using previously tested rectangular specimens as the material for the new ones, the thermocouple placement and surface finish were preserved; thereby allowing a comparison based on geometry alone. As these circular specimens were cut from one end of the rectangular ones, only three thermocouples were used to determine the temperature gradient in the specimens. A drawing of the circular specimen showing dimensions and thermocouple location is shown in Figure 3. Figure 4 shows the thermocouples in place in the specimen.

B. Mounting Block for Test Specimen.

Details of the mounting block construction can be seen in Figures 5 and 6 which are scale drawings and in the photograph, Figure 7. In general, it is a rectangular box with sides and bottom of 1/4" aluminum sheet and a top of 1/2" aluminum sheet. This box is lined with 1/4" Teflon sheet. The coil for heating the test specimen is wound in a groove in a Lavite block, 4-3/4" x 1-1/2", on which the specimen is placed. A fire brick, 6" x 4-1/2" x 2-1/2" was milled to hold the Lavite block. The space between the Teflon lining and the fire brick was filled with flaked asbestos insulation. The Teflon and aluminum tops have a "window", 2" x 3-1/2", cut in them so that the test specimen will be in contact with the distilled water. There are also four 1/2" copper tubes attached to the top of the box for power and thermocouple leads. These tubes extend well above the surface of the water to insure water tightness of the box. The top is gasketed around both the outside perimeter and the "window" with Neoprene gaskets. Water tightness is insured by clamping the top to the box with two aluminum bars, 1/2" x 1" x 9-1/2", and four stainless steel studs. These studs and bars are not shown in the cross sectional views to avoid confusion but their position may be seen in the photograph, Figure 8.

For testing the circular specimens, the mounting block was modified by putting on a new aluminum top plate with Teflon liner both with a circular window, 2 inches in diameter, to permit specimen contact with the distilled water.

The mounting block is contained in a Pyrex jar, 12 inches in diameter and 12 inches high, filled to a depth of 9 inches with distilled water.

C. Temperature Measurement.

Six thermocouples were placed in each specimen: four, 1/16 inch below the test surface and two, 1/8 inch above the lower surface. The exact positioning is shown in Figures 9 and 10. This placement proved satisfactory since a sufficient number of points were available to establish a temperature gradient so that test surface temperature could be obtained by extrapolation. Brown and Sharpe #30 gauge, iron-constantan, duplex, glass insulated thermocouple wire was used.

The thermocouple holes were partially filled with "Eccobond" Solder 57C to insure good thermal and electrical contact with the specimen. As a cement and to provide further thermal contact the thermocouples were held in place with Insa-lute Hi-Temp Cement #P-1 made by the Sauerseisen Cement Company. The thermocouple leads were taken to a terminal board from which the signal was transmitted to a thermocouple switch by means of Brown and Sharpe #24 gage, iron-constantan thermocouple wire. The thermocouples were referenced to a common ice junction and the selector switch was connected so that the temperature at each location could be read separately. The reading of the potential of the thermocouples was obtained with a Rubicon Precision Potentiometer Model #2732. A wiring diagram is shown in Figure 11.

In addition to the specimen thermocouples, four were placed on the outside of the mounting block to estimate heat loss through the box. One thermocouple was placed on the top, one on the bottom and one on each of two vertical perpendicular sides. These thermocouples were made from Brown and Sharpe #24 gage wire and were peened into the aluminum plate of the mounting block. The temperature of the distilled water was measured with a mercury in glass, 0-220°F, thermometer suspended 1/2" above the test surface.

D. Power Supply and Measurement.

Heat was supplied to the test specimen from a nichrome wire heating coil wound as shown in Figures 12 and 13. Figure 12 is for rectangular specimens and Figure 13 for circular ones. The coil was made by Hoskins Manufacturing Company, size #FD 101, 110V, using Brown and Sharpe #20 gage wire. The room temperature resistance of the rectangular coil was 20.0 ohms; the circular one, 10 ohms. Power was supplied to the heating coil from a 220 volt, single phase source through a 230 volt, 8 amp Variac, Type V20HM, manufactured by General Radio Company. Voltage drop across the coil and current passing through the coil were measured by a Style #701350 ammeter and a Style #701329 voltmeter manufactured by Westinghouse Electric and Manufacturing Company. A wiring diagram is shown in Figure 14. To maintain the distilled water near boiling temperature throughout a test-run, the water was heated by a Calroc heater, immersed in the bath.

E. Surface Roughness Equipment.

Roughness of the specimen heating surface was measured with a Brush Model BL-103 Surface Analyzer [16]. The equipment consists essentially of four components: a motor driven pick-up arm, a calibrating amplifier, an averaging meter and a direct inking oscillograph. The pick-up arm contains a 0.0005 inch diamond stylus attached to a crystal. The arm is driven by the drive motor and moves back and forth through a ten second cycle. The vertical motion of the diamond stylus as it travels over the surface causes the crystal to be bert. This produces an emf which is proportional to the amount of vertical motion of the arm. This voltage is amplified in the calibrating amplifier and drives the pen motor of the oscillograph. The chart of the oscillograph records in micro-inches the direction, magnitude and regularity of surface roughness. The averaging meter can be used to give a visual indication of root mean square values of the roughness. Since the roughness of the specimens was not held to extremely close tolerances, the averaging meter was used to indicate the relative order of increasing roughness of the specimens. The Brush Surface Analyzer equipment arrangement can be seen in Figure 15.

CHAPTER III

EXPERIMENTAL PROCEDURE

The supplementary Calrod heater was turned on and the distilled water bath allowed to heat up to 160°F before the mounting block containing the test specimen was lowered into place. The test specimen heating surface was cleaned with acetone prior to assembly of the test specimen mounting block to remove all grease and other foreign matter. With the test specimen in place, the maximum power, approximately 0.8 kw, was applied to the specimen heating coil and the entire system allowed to reach steady state condition. The maximum power was dictated by the heating coil kw rating. This usually required 30-45 minutes to reach the boiling point of the water bath and another two to two and one-half hours of vigorous boiling for steady state. The water level in the test tank was maintained constant by introducing previously heated distilled water into the test tank below the mounting block so as not to disturb the convection currents in the vicinity of the test specimen. When steady state was reached with maximum power input, all necessary readings were taken. A sample data sheet is shown in Table II of Appendix B. The power input was lowered in approximately equal steps and readings taken when successive steady state points were reached. Power was lowered until boiling from the test surface ceased. It required approximately one hour to reach steady state at each test point so that a total run time of ten hours resulted.

SURFACE ROUGHNESS MEASUREMENT

Surface roughnesses were indicated by two methods. Before testing of the specimens they were sent to the machine shop with a shop drawing

specifying the finish desired. The usual practice of the machine shop is to use a visual comparison with a "standard" surface to determine the finish obtained. Machining is continued until the desired finish is reached. In this case the "standard" surface used was a General Electric Corporation "Surface Roughness Scale" Catalogue No. 8665947-G1.

In addition the "Tracer method" which employes a stylus that is dragged across the surface was used. The "Brush Surface Analyzer" as described in Chapter II proved satisfactory for this purpose. According to Bechwith and Buch [17], this is the most common method for obtaining quantitative results.

There are several problems with this type of equipment. First, in order for the scriber to follow the contour of the surface it should have as sharp a point as possible. If irregularities are smaller than the size of the point used, the stylus, being of a very hard material, usually diamond, will round off the peaks as it is dragged over the surface. It will actually cut a groove in the surface being measured. Grooves were observed in the smoother surfaces however, this had no effect on the results of the experiment for as Corty and Foust [4] observed, no preferential nucleation was ever noticed along such marks.

In spite of its inherent inaccurancies, the "Tracer method" is the most used and is reproducible for a given material.

For the "Tracer method", roughness readings were taken at nine locations as shown in Figure 16. The lowest and highest readings at each location, as indicated by the averaging meter (rms), were recorded. The nine high and low readings were averaged to give the roughness values listed in Table I.

CHAPTER IV

DISCUSSION OF RESULTS AND CONCLUSIONS

The significant parameters used in presenting the results of this experiment are t_s, average heating surface temperature, q/A, heat rate, and t_w, bulk temperature of the distilled water. Since it was not possible, with the apparatus used, to maintain the water at the saturation temperature at all times, the bulk water temperature was used in calculating Δt_m. The degree of subcooling reaching a maximum of 4°F at the low heat rates.

The method of obtaining the parameters was as follows: t_w was measured with a mercury thermometer; an average temperature gradient in the specimen was obtained from the imbedded thermocouples and t_s was calculated by extrapolation; using published k, thermal conductivity, data and the average temperature gradient, q/A was calculated.

The results of the investigation are presented giving the variation of heating rate, q/A, as a function of Δt_m for the various surface roughnesses. The results are presented in two forms: graphical, Figures 17 through 40, and tabular, Table III. A sample calculation of results for Run #7 is given in Appendix B.

When dealing with extremely rough surfaces, the size of the irregularities is such that a significant difference in temperature may exist between the base and the tip of the irregularities. Since the surface temperature is used in calculating Δt_m, a decision must be made as to whether to use the temperature at the base or the tip or at a point between. The temperature used in this thesis was that at the base as determined by extrapolation using the temperature gradient between the two thermocouple levels. In order to determine whether this introduces a significant difference in

Δt_m, depending on whether the temperature at the base or that at the tip is used, calculations were performed as shown in Appendix B. Equation (2-56) page 55 of Kreith [18] was used for this calculation.

For specimens #1 and #2, which were extremely rough, there was a significant difference, the maximum difference for specimen #1 being 0.4°F for a 5.7°F Δt_m, indicating that it is important to specify the location of surface temperature for rough specimens. For other specimens, where finishes were measured in micro inches, the difference between base and tip temperatures was insignificant as can be seen by examining the order of magnitude of L in the above equation. Therefore, no correction was made in the extrapolated temperature for these specimens.

Figure 17 is a composite plot of all rectangular specimens tested while Figures 18 and 19 show the comparison between a rectangular and a circular specimen with the same surface finish. Figures 20 and 21 are for duplicate tests on the same specimens on succeeding days for determining reproducibility of data. Specimens #1 and #2, with deep grooves machined in the surfaces, were tested and the results are given in Figure 22. The remaining Figures, 23 thru 36, are for each individual run. Experimentally determined points are plotted and with them are shown the uncertainty that exists in both co-ordinates. The method of determining this uncertainty is discussed later in this chapter under Experimental Accuracy.

As can be seen from Figure 17, heat rates, q/A, vary from a maximum of about 29,000 Btu/hr ft^2 to a minimum of 3000 Btu/hr ft^2 while temperature difference between the heating surface and the water varies from 39° to 0.5°F. Following is a table showing the ranges of heat rate, q/A, and Δt_m for the various roughnesses tested. Also listed are the figures in which the results for that roughness are plotted.

Figure	Roughness	Heat Rate $\frac{Btu}{hr\ ft^2}$	Δt_m °F
23	.008 in.	27,600-8580	5.7-1.7
24	.005 in.	28,200-4550	5.9-0.6
25	84-109 μin.	24,800-3070	16.5-7.3
26	40-52 μin.	25,500-3000	16.8-8.6
27	28-37 μin.	25,400-3220	16.0-5.9
28	22-24 μin.	28,200-4040	22.3-5.4
29	13-17 μin.	28,000-4340	24.3-7.5
30	3.6-8.2 μin.	21,600-4130	27.0-10.4
31	4.5-6.2 μin.	20,900-2525	33.0-12.4
32	2.2-4.0 μin.	24,100-3820	39.1-19.1

In addition to Figure 17 in which the results of tests on all surface roughnesses are presented as q/A versus Δt_m, these results are also presented on a log-log plot of q/A vs. Δt_m in Figure 39 and as h vs Δt_m, also log-log, in Figure 38.

EXPERIMENTAL ACCURACY

The technique used in determining the uncertainties in the experimental values of q/A and Δt_m is that described by Kline and McClintock [20] An uncertainty as defined by them is the possible value the error might have.

> "For a single observation, the error, which is the difference between the true and observed values, is a certain fixed number. But the uncertainty, or what one thinks the error might be, may vary considerably depending upon the particular circumstances of the observation."

In this case the uncertainties in the measured values of specimen temperature as indicated by thermocouple readings were assumed as the maximum possible value that could exist for that run. Using the data from Run #7, a calculation is given in Appendix B illustrating the method used in determining the uncertainties plotted in Figures 23 thru 36. The uncertainties vary slightly from specimen to specimen; however, in general, the uncertainty in Δt_m varies from $\pm$ 3.0 °F at high heat rates to $\pm$ 0.5 °F at low ones while that of q/A varies from $\pm$ 1500 Btu/hr ft^2 at high values to $\pm$ 150 Btu/hr ft^2 at low ones.

CONCLUSIONS

The results of these tests show that surface roughness has a pronounced influence on the rate of heat transfer from a stainless steel (Type 304), horizontal plate to distilled water in the nucleate boiling regime. For very smooth surfaces the Δt_m or temperature driving potential necessary to maintain a specified heat rate is especially sensitive to changes in surface finish. However, as roughness increases, the Δt_m for a given heat rate decreases at a slower rate. This implies a roughness limit above which surface roughness has little effect on Δt_m. As can be seen from Figure 37, a plot of Δt_m vs. roughness for a given heat rate, q/A, the order of magnitude where this occurs is about 25 to 30 μin rms. which agrees with the results of Corty and Fousts' [4] work with N-Pentane and nickel. Figure 40 shows a comparison between the above work and this experiment for a surface coefficient, h, of 1000 Btu/hr ft^2°F. Figure 37 also shows clearly the decrease of the Δt_m as roughness increases with a constant q/A. For example for a heat rate of 20,000 Btu/hr ft^2 Δt_m was 36.5°F for a roughness of 3.1 μin rms. and decreased to 17.5°F at 23 μin. rms.

It can also be seen that the slopes of the q/A vs. Δt_m curves vary with roughness. As the roughness increases the slope also increases indicating that extremely high heat rates may be obtained using "rough" materials while maintaining a low value of Δt_m.

The specimens used in this experiment were finished using normal machining operations. Therefore, the shape of the irregularities in the test surfaces would vary from specimen to specimen. It is fairly well accepted by other investigators that both size and shape of these irregularities affect heat transfer characteristics. Since each specimen was prepared with different machining operations, it appears that size or roughness is more influential than shape in affecting these characteristics.

The results of the tests with circular specimens indicate that the geometry of the test specimen had little effect on the results of this experiment. This is as should be expected if the theory proposed by most investigators in this field, that the heat transfer rate is actually a function of the number of nucleating sites, is accepted. The number of sites then, as a function of the surface finish, should not change with geometry.

The curve of Figure 22 for specimens #1 and #2 indicate that heat transfer rates are highly sensitive to small changes in Δt_m for these rough finishes. The calculation of q/A was handled the same way for both types of surface finish, micro and macro roughness; the projected horizontal area was considered as the heat transfer area. When dealing with a surface with deep grooves, there is actually a roughness associated with the sides of the grooves as well as an overall roughness of the specimen. Again following the theory that heat transfer rate, q/A, is a function of the number of nucleating sites, extremely rough surfaces would present more

sites per unit projected area than a relatively smooth surface. Therefore, it would be expected that for a given q/A the Δt_m would be lower.

BIBLIOGRAPHY

1. Kurikara, H. M. and Myers, J. E., "The Effects of Superheat and Surface Roughness on Boiling Coefficients," A.I. Ch. E. Journal, March, 1960, p. 83.

2. HSU, S. T. and Schmidt, F. W., "Measured Variations in Local Surface Temperatures in Pool Boiling of Water," Transactions of ASME, August 1961. Vol. 83, Series C., No. 3., p. 254.

3. Griffith, P. and Wallis, J. C., "The Role of Surface Conditions in Nucleate Boiling." A.I. Ch.E., Chemical Engineering Progress Symposium Series No. 30, 1960, Vol. 56, p. 49.

4. Corty, C. and Foust, A. S., "Surface Variables in Nucleate Boiling," A.I. Ch.E., Chemical Engineering Progress Symposium, Series No. 17. 1955, Vol. 51, p. 1.

5. Lummis, R. C., "An Experimental Study of the Transient Vaporization of Liquid at a Solid Surface," Basic Studies in Heat Transfer and Fluid Flow, Quarterly Progress Report for period, April 1, 1960 to June 30, 1960. Engineering Research Laboratories, Columbia University, N. Y., U.S.A.E.C. TID-6035 p. 21.

6. Stock, B. J., "Observations on Transition Boiling Heat Transfer Phenomena." Argonne National Laboratory, ANL 6175, June 1960.

7. Gunther, F. C., 'Photographic Study of Surface-Boiling Heat Transfer with Forced Convection", Trans. Am. Soc., Mech. Engrs. 73, 115 (1951).

8. Rohsenow, W. M. and J. A. Clark., "A Study of the Mechanism of Boiling Heat Transfer", Trans. Am. Soc. Mech. Engrs. 73, 609 (1951).

9. Perkins, A. S. and J. W. Weswater, "Measurements of Bubbles formed in Boiling Methanol," presented at meeting of Am. Inst. of Chem. Engrs. New Orleans, La., May 8, 1956.

10. McAdams, W. H., "Heat Transmission", McGraw-Hill Book Co., 3rd Ed., 295, 1942.

11. Jakob, M., "Temperature, its Measurement and Control in Science and Industry," Reinhold, New York, 1941.

12. Kreith, F. and Summerfield, M., Trans. Am. Soc. Mech. Engrs. 72, 869, 1950.

13. Bankoff, S. G. "The Entrapment of Gas in the Spreading of a Liquid over a Rough Surface", presented at Am. Inst. of Chem. Engrs. New Orleans, La., May 8, 1956.

14. Gaertner, R. F., and Westwater, J. W., "Population of Active Sites in Nucleate Boiling Heat Transfer," Am. Inst. of Chem. Engrs. Chemical Engineering Progress Symposium, Series Number 30, 1960, Vol. 56.

15. Kurikara, H. M., "Fundamental Factors Affecting Boiling Coefficients," PhD Thesis, Purdue University, Lafayette, Indiana, 1956.

16. "Operating Instructions of Brush Model BL-103 Surface Analyzer," Brush Electronics Co., Cleveland, Ohio.

17. Beckwith, T. G., and N. Lewis Buck, Mechanical Measurements, Addison-Wesley Publishing Co., Inc., Reading, Mass., 1961.

18. Kreith, Frank, Principlas of Heat Transfer, International Textbook Co., Scranton, Pennsylvania.

19. Metals Handbook

20. Kline, S. J., and McClintock, F. A., "Describing Uncertainties in Single-Sample Experiments", Mechanical Engineering, Jan. 1953.

APPENDIX A

TABLE III

EXPERIMENTAL RESULTS

Run #	Δt_m °F	dt/dx °F/in.	q/A Btu/hr ft^2	h Btu/hr ft^2 °F	Specimen #
11	16.5	220.0	24800	1502	3
	15.8	165.6	18680	1181	
	13.1	113.3	12800	977	
	11.8	66.1	7450	631	
	7.8	35.8	4040	518	
	7.3	27.2	3070	421	
10	24.5	265.0	29900	1220	7
	20.9	214.0	24150	1155	
	16.6	139.8	15780	950	
16	24.3	248.5	28100	1155	7
	21.0	191.2	21600	1030	
	15.9	117.0	13200	830	
	12.1	69.6	7850	648	
	7.5	38.4	4340	578	
7	16.0	225.0	25400	1588	5
	15.4	173.0	19500	1267	
	13.6	135.0	15300	1125	
	11.6	90.0	10150	875	
	9.3	55.2	6230	670	
	5.9	28.5	3220	546	
5	33.0	185.3	20900	634	9
	30.2	155.4	17530	580	
	26.4	126.0	14200	538	
	23.7	84.3	9500	401	
	18.7	56.9	6420	343	
	15.7	25.1	2830	180	
	12.4	22.4	2525	203	

Run #	Δt_m °F	dt/dx F/in.	q/A Btu/hr ft^2	h Btu/hr ft^2 °F	Specimen #
9	27.0	191.5	21600	800	8
	22.3	123.0	13880	622	
	18.2	85.7	9660	530	
	14.0	51.3	5780	412	
	10.4	36.6	4130	397	
18	5.9	250.0	28200	4780	2
	4.3	193.0	21750	5060	
	3.2	139.0	15690	4900	
	1.8	79.7	9000	5000	
	0.6	40.3	4550	7580	
24	6.9	296.0	33400	4840	1
	5.7	245.0	27600	4840	
	4.0	180.0	20300	5070	
	2.7	117.8	13280	4920	
	1.7	76.1	8580	5040	
28	34.6	184.8	20850	602	9 (Circular)
	30.1	139.5	15730	523	
	25.3	91.4	10300	407	
	20.1	55.0	6200	308	
29	23.8	268.0	30200	1268	6 (Circular)
	20.0	193.8	21850	1092	
	15.6	131.0	14780	947	
	10.8	78.9	8900	824	
14	25.2	181.0	20400	809	8
	22.0	135.5	15300	696	
	17.7	94.2	10620	601	
	13.6	57.5	6480	477	

Run #	Δt_w °F/in.	dt/dx Btu/hr ft^2	q/A Btu/hr ft^2	h Btu./hr. ft^2 °F	Specimen #
12	16.8	226.0	25500	1518	4
	14.7	156.0	17600	1197	
	12.5	95.7	10800	864	
	10.0	59.0	6660	666	
	8.6	26.6	3000	349	
17	22.3	249.5	28200	1263	6
	18.2	181.0	20400	1120	
	14.4	123.4	13920	967	
	10.1	67.8	7650	758	
	5.4	35.8	4040	748	
15	39.1	213.5	24100	617	10
	34.9	152.4	17200	493	
	30.8	110.5	12490	405	
	25.0	64.8	7310	292	
	19.1	33.8	3820	200	

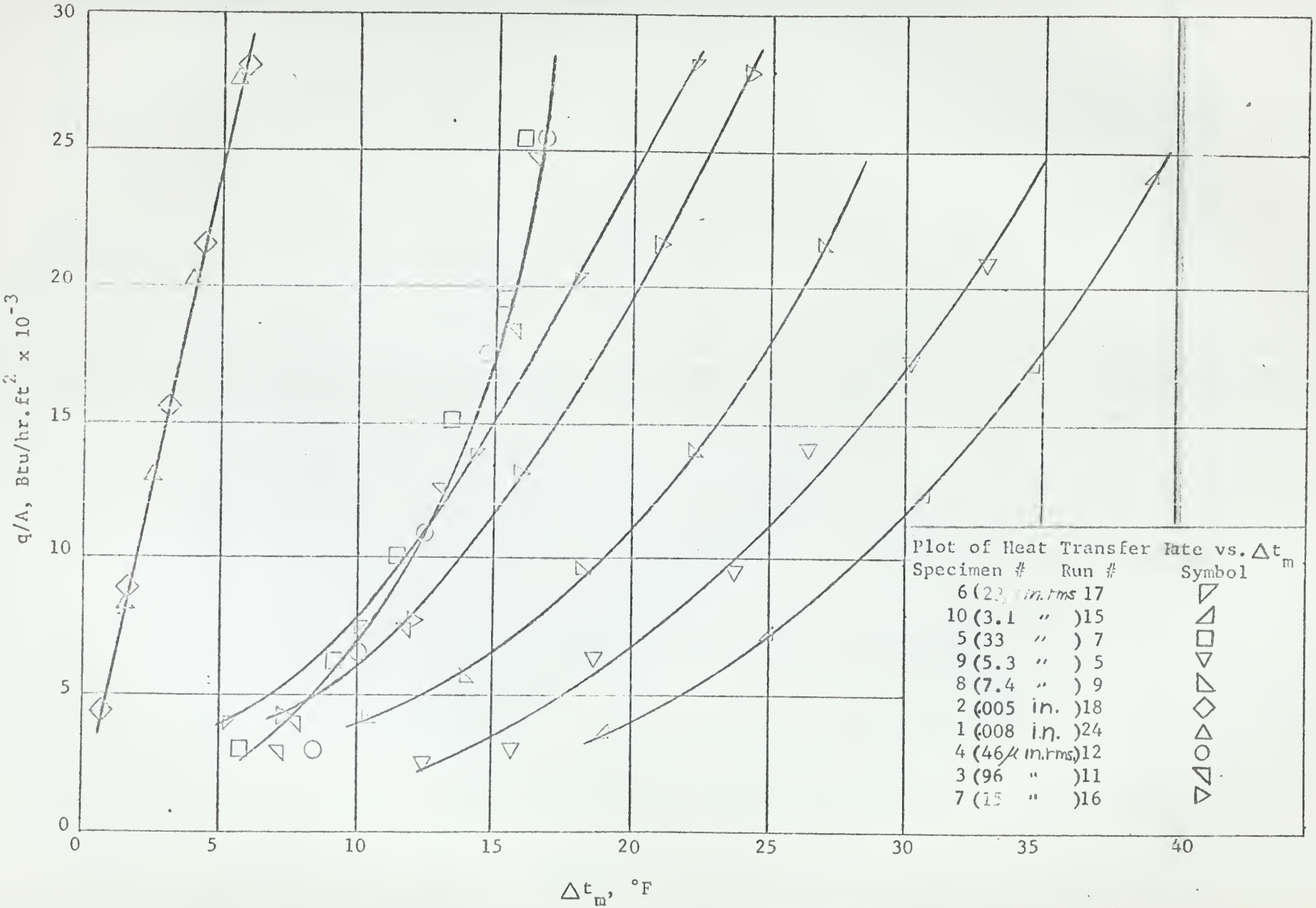
30
25
20
15
10
5
0
0
5
10
15
20
25
30
35
40
q/A, Btu/hr.ft^2 x 10^{-3}
Δt_m, °F
Plot of Heat Transfer Rate vs. Δt_m
Specimen # Run # Symbol
6 (23 μin.rms 17
10 (3.1 ")15
5 (33 ") 7
9 (5.3 ") 5
8 (7.4 ") 9
2 (.005 in.)18
1 (.008 in.)24
4 (46μ in.rms)12
3 (96 ")11
7 (15 ")16

FIGURE 17

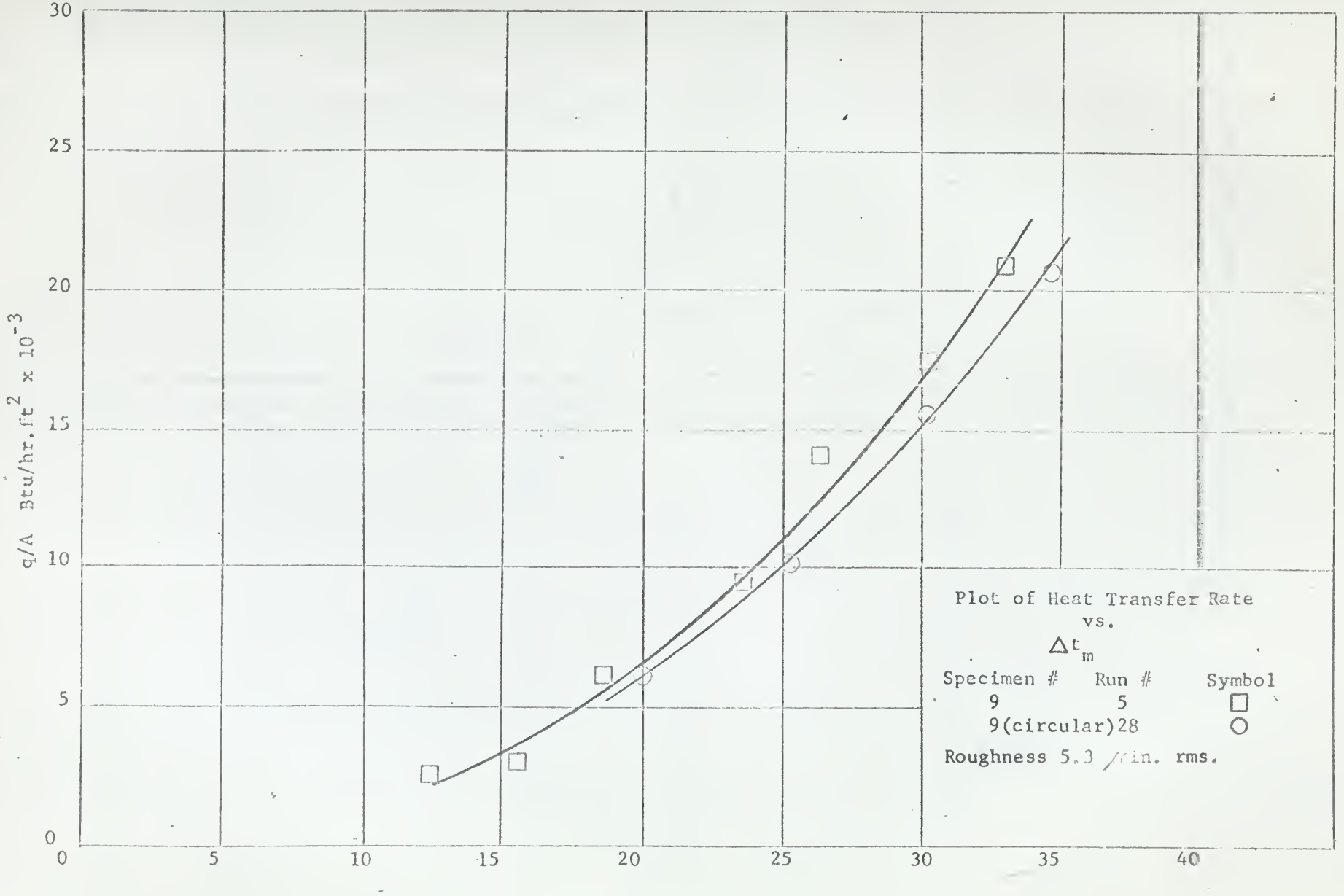
30
25
20
15
10
5
0
0
5
10
15
20
25
30
35
40
q/A Btu/hr.ft^2 x 10^{-3}
Δt_m °F
Plot of Heat Transfer Rate
vs.
Δt_m
Specimen # Run # Symbol
9 5
9(circular) 28
Roughness 5.3 µin. rms.

FIGURE 18

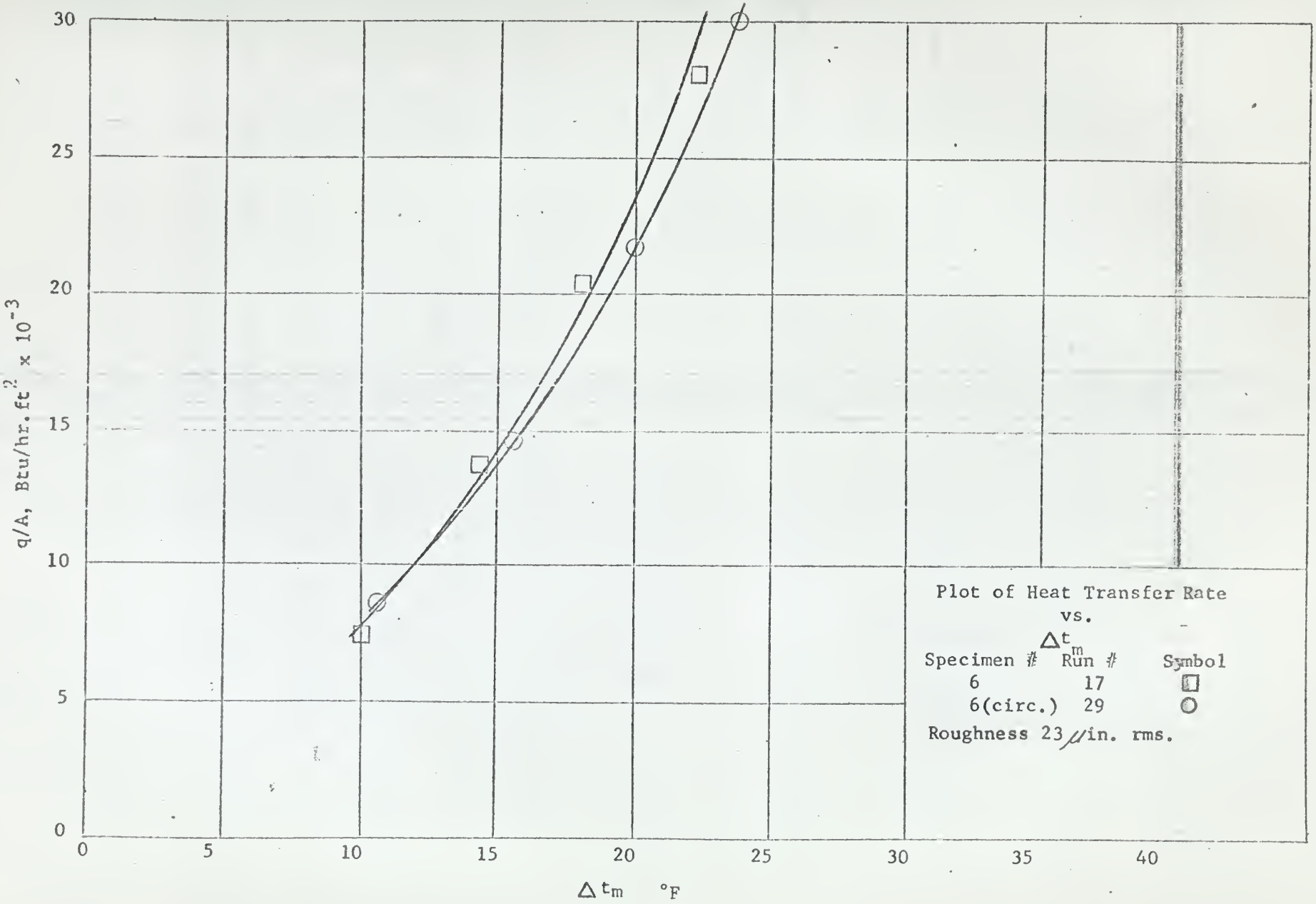
30
25
20
15
10
5
0
0
5
10
15
20
25
30
35
40
q/A, Btu/hr.ft² x 10⁻³
Δ tm °F
Plot of Heat Transfer Rate
vs.
Δtm
Specimen # Run # Symbol
6 17
6(circ.) 29
Roughness 23 μin. rms.

FIGURE 19

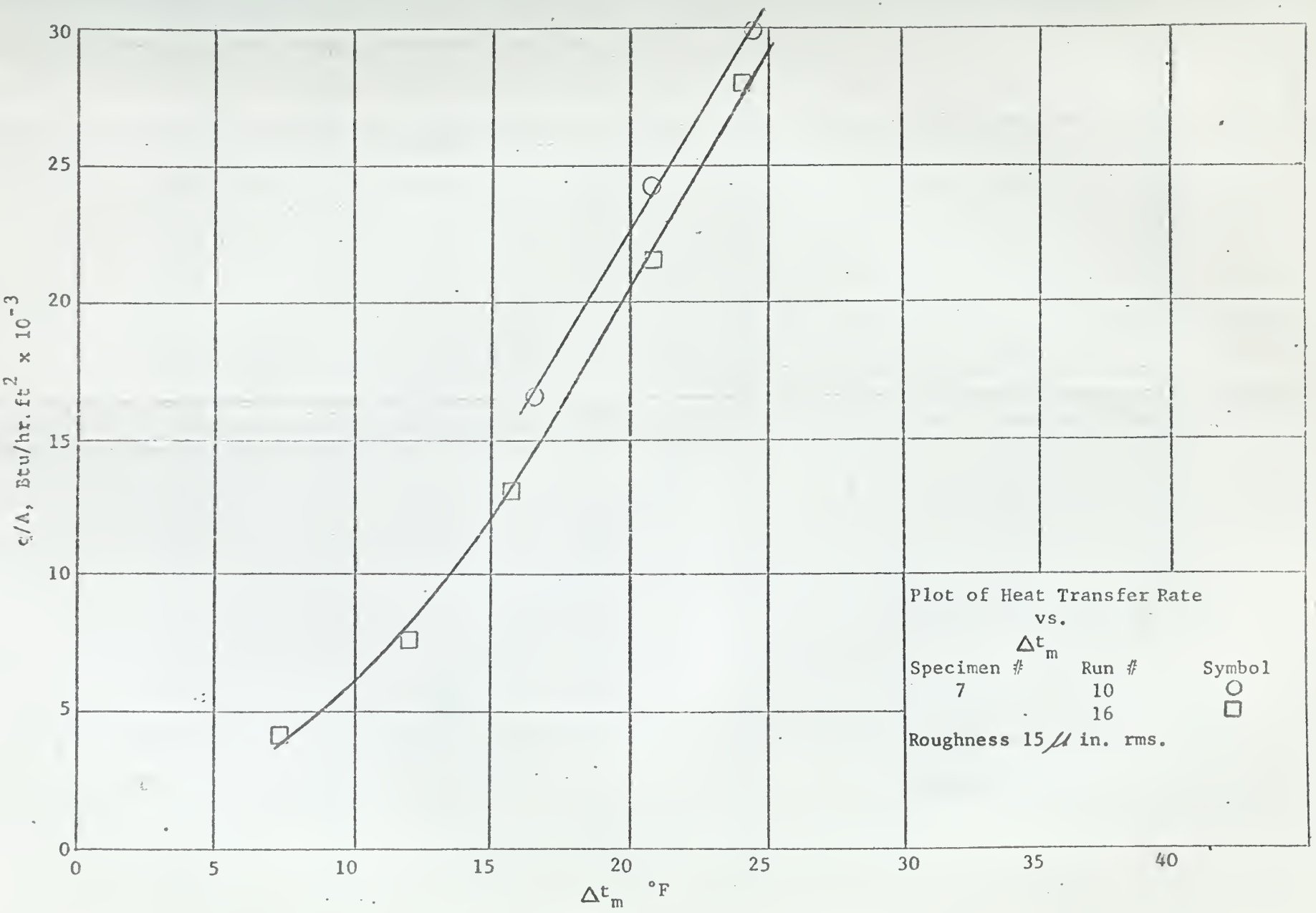
30
25
20
15
10
5
0
0
5
10
15
20
25
30
35
40
q/A, Btu/hr.ft^2 x 10^{-3}
Δt_m °F
Plot of Heat Transfer Rate
vs.
Δt_m
Specimen # Run # Symbol
7 10
16
Roughness 15 μ in. rms.

FIGURE 20

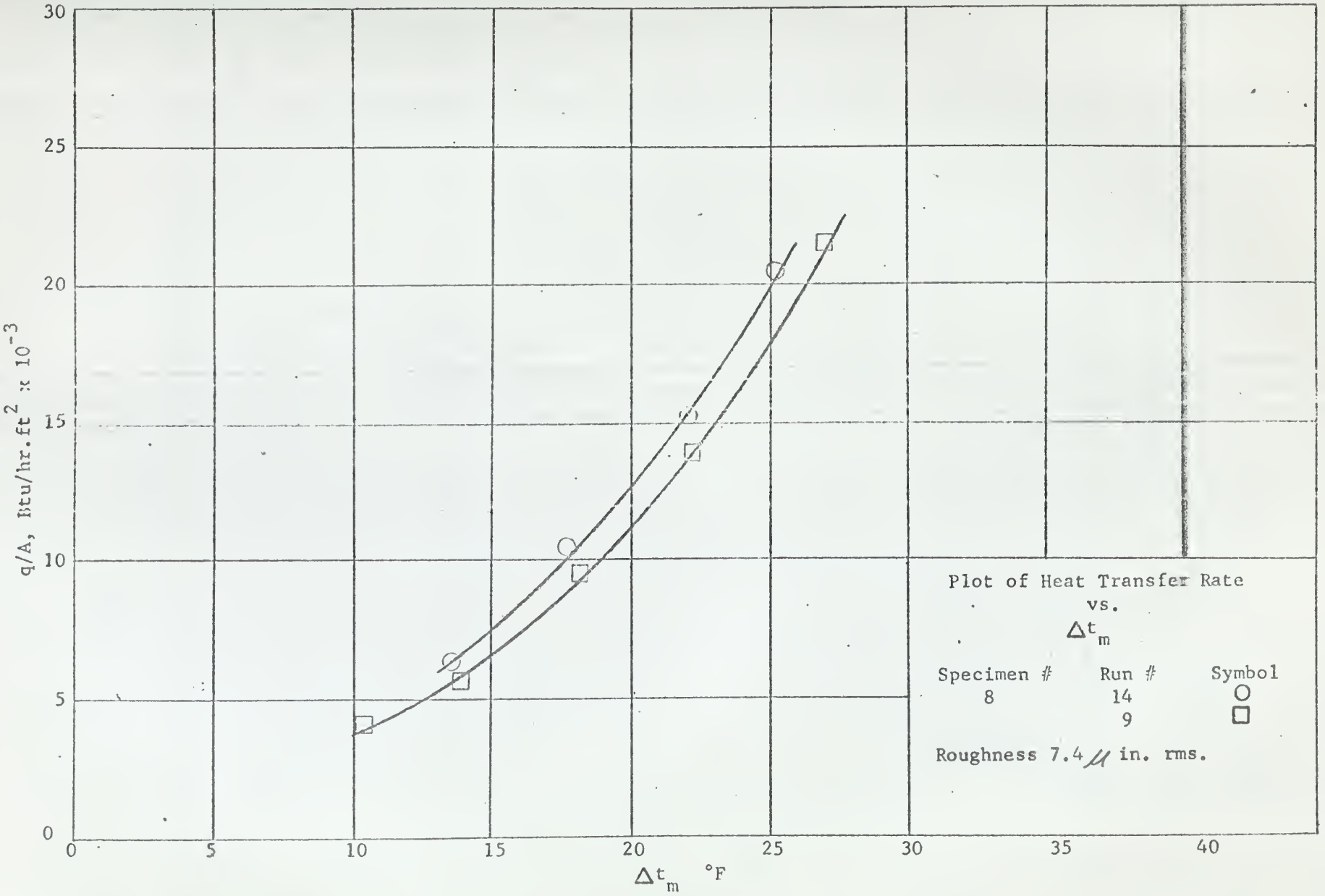
30
25
20
15
10
5
0
0
5
10
15
20
25
30
35
40
q/A, Btu/hr.ft^2 x 10^{-3}
Δt_m °F
Plot of Heat Transfer Rate
vs.
Δt_m
Specimen # Run # Symbol
8 14 ○
9 □
Roughness 7.4 μ in. rms.

FIGURE 21

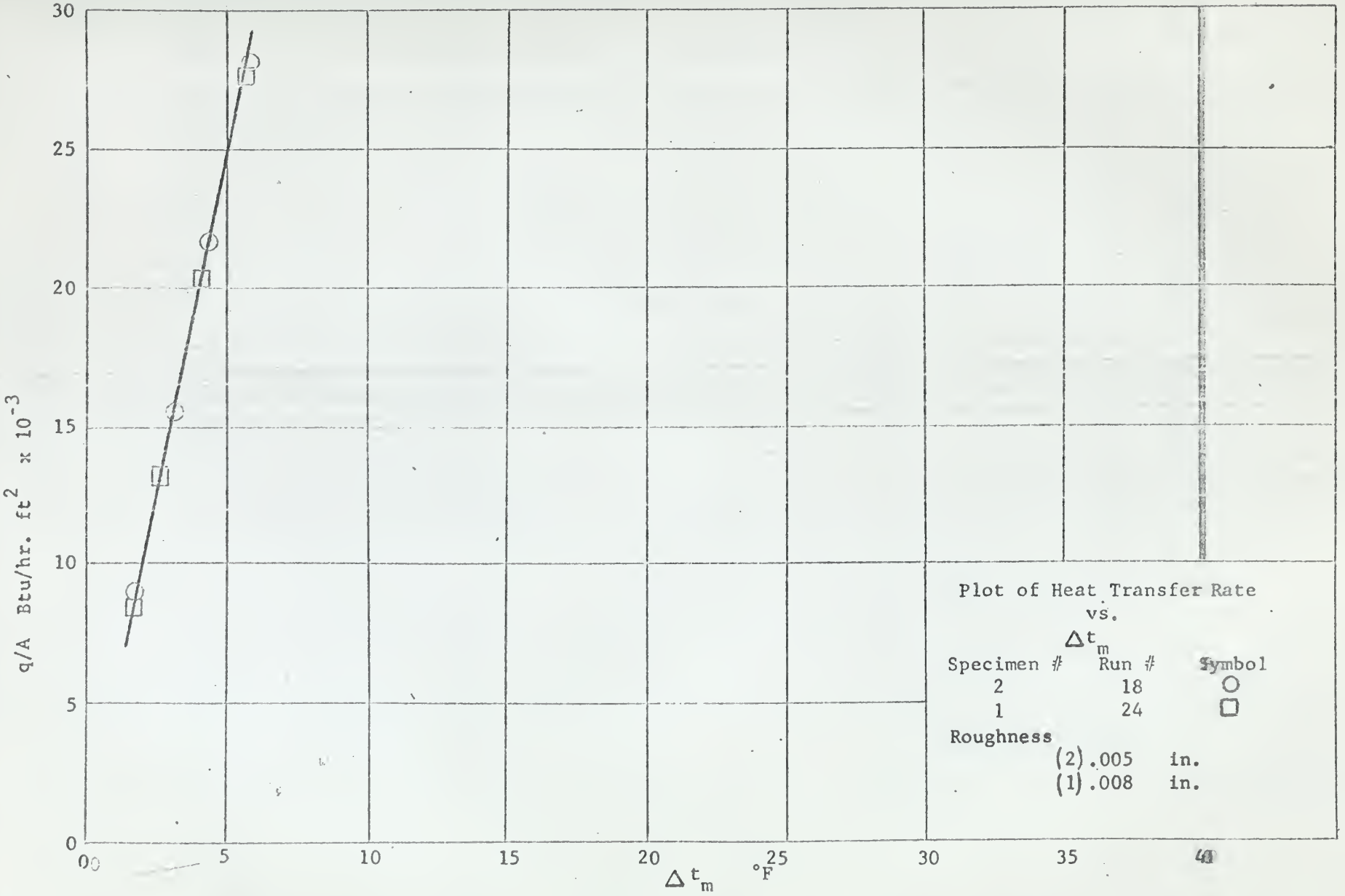
30
25
20
15
10
5
0
q/A Btu/hr. ft^2 x 10^{-3}
0
5
10
15
20
25
30
35
40
Δt_m °F
Plot of Heat Transfer Rate
vs.
Δt_m
Specimen # Run # Symbol
2 18 ○
1 24 □
Roughness
(2) .005 in.
(1) .008 in.

FIGURE 22

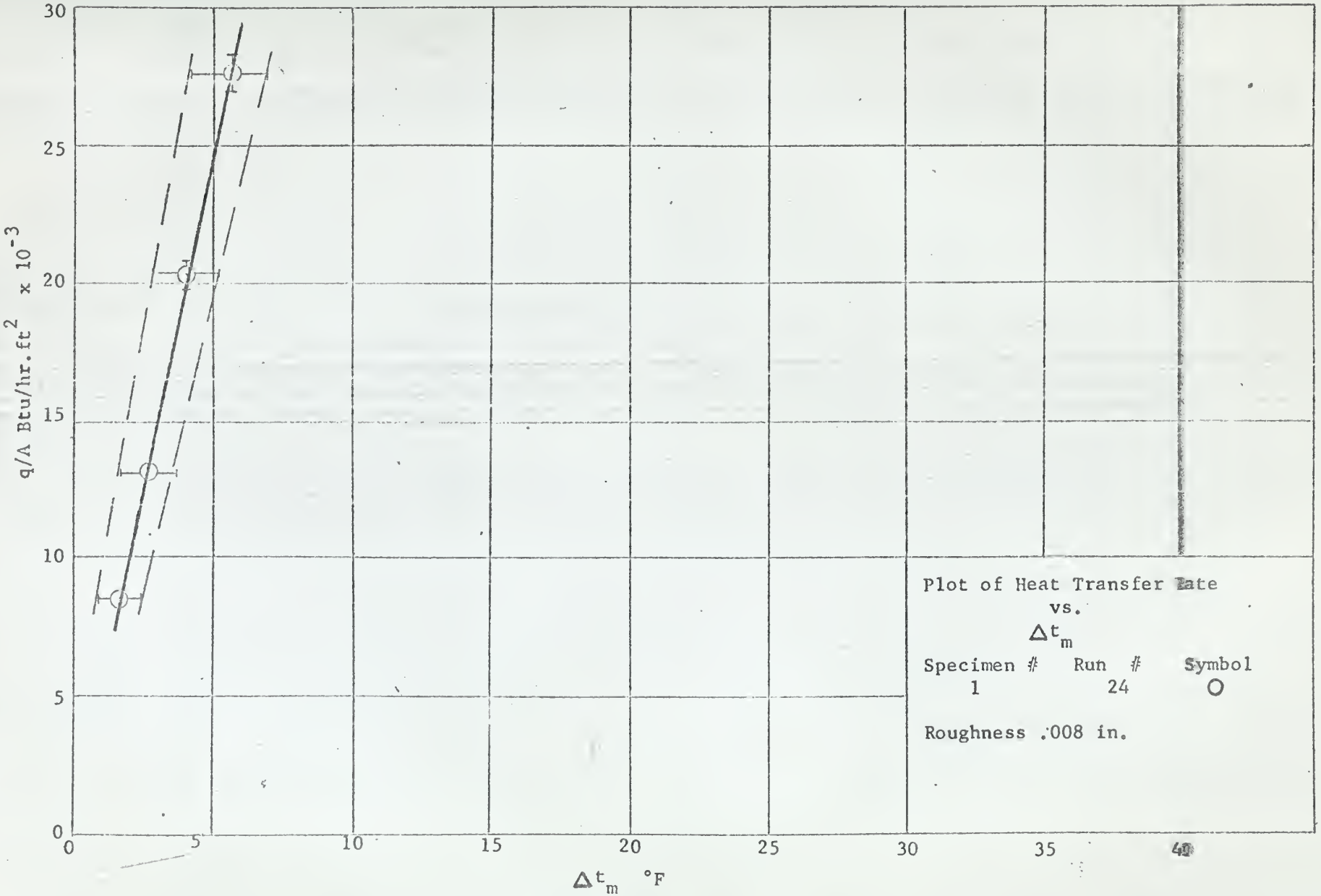
30
25
20
15
10
5
0
q/A Btu/hr.ft^2 x 10^{-3}
0
5
10
15
20
25
30
35
40
Δt_m °F
Plot of Heat Transfer Rate
vs.
Δt_m
Specimen # Run # Symbol
1 24 O
Roughness .008 in.

FIGURE 23

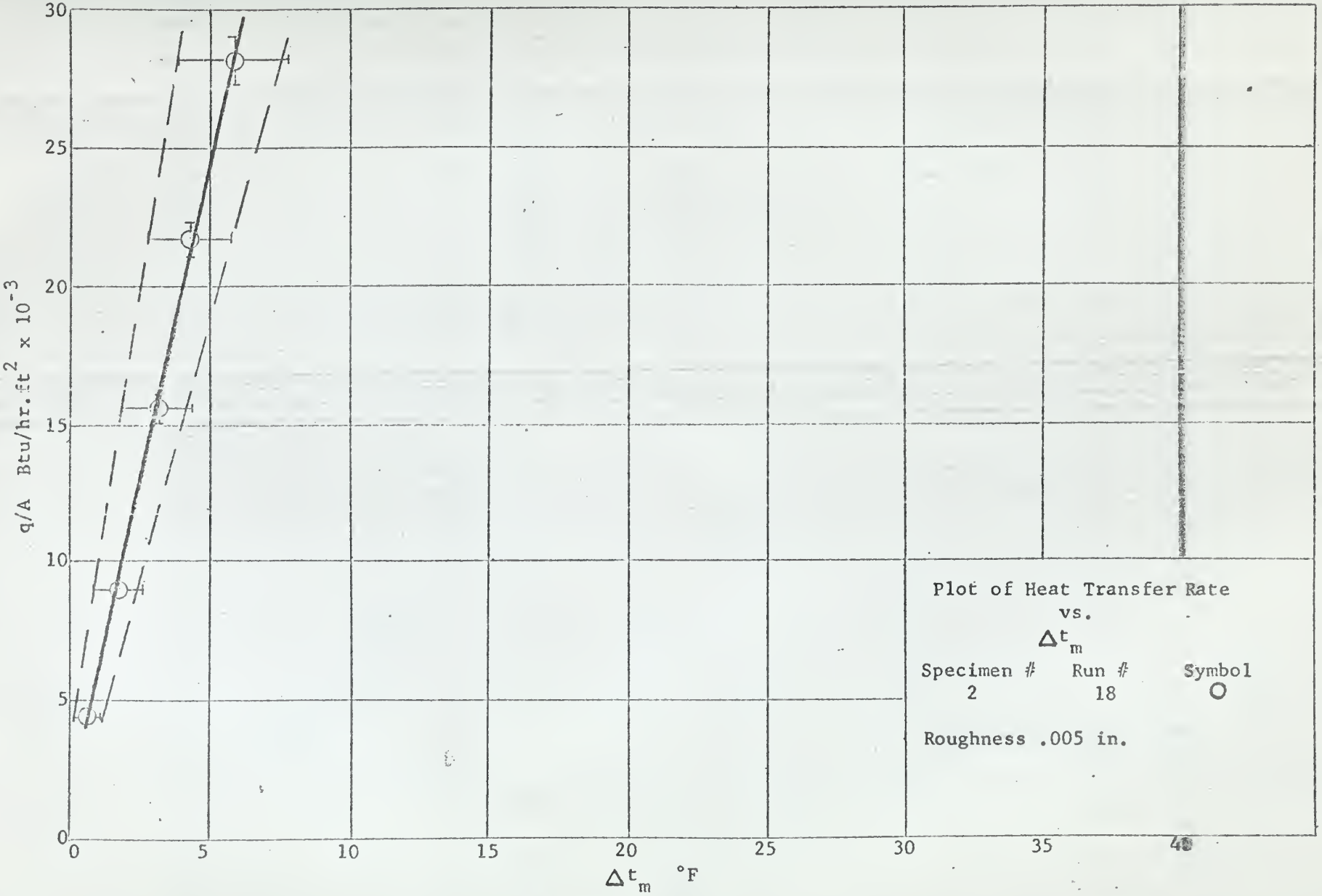
q/A Btu/hr.ft^2 x 10^{-3}
30
25
20
15
10
5
0
0
5
10
15
20
25
30
35
40
Δt_m °F
Plot of Heat Transfer Rate
vs.
Δt_m
Specimen # 2
Run # 18
Symbol O
Roughness .005 in.

FIGURE 24

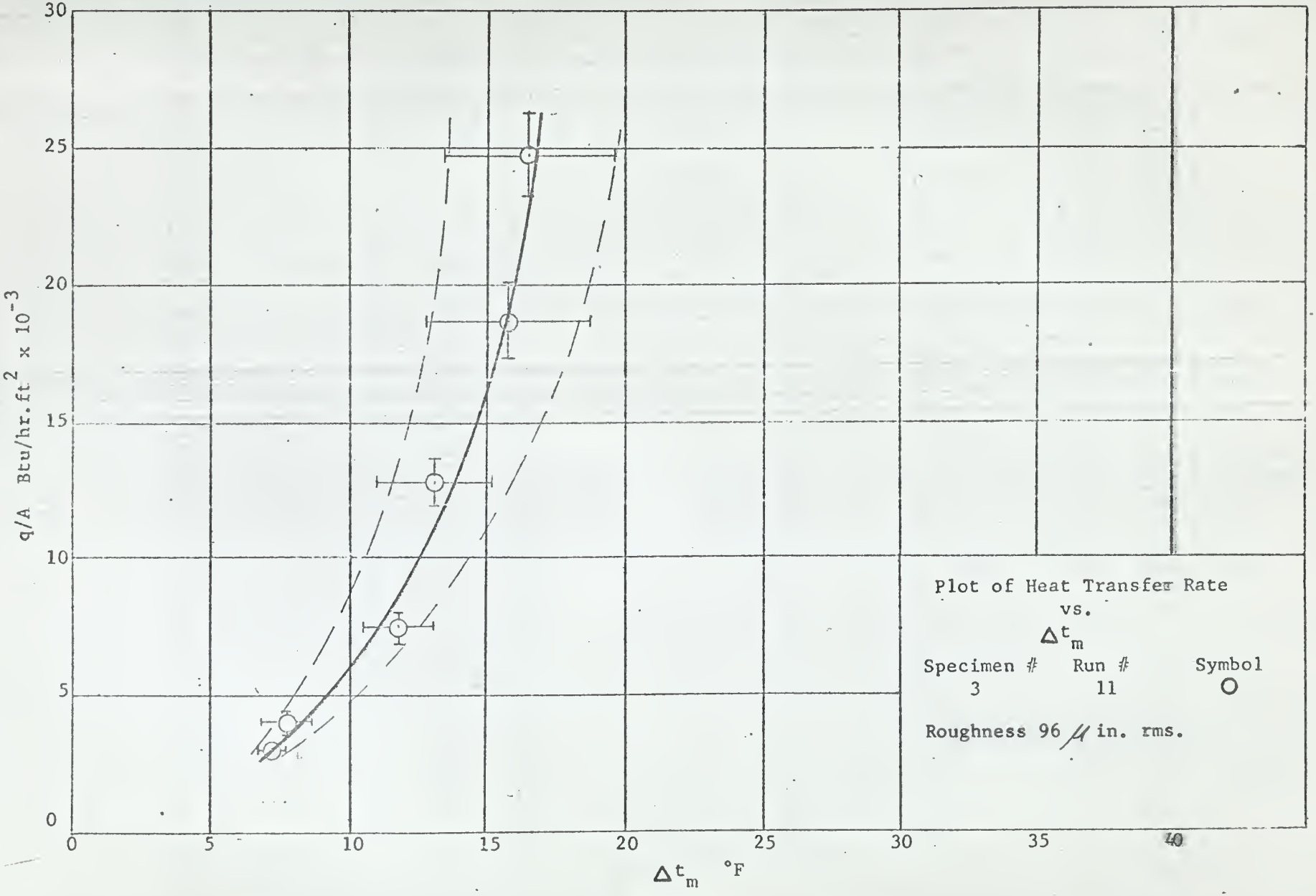
30
25
20
15
10
5
0
q/A Btu/hr.ft^2 x 10^{-3}
0
5
10
15
20
25
30
35
40
Δt_m °F
Plot of Heat Transfer Rate
vs.
Δt_m
Specimen # 3
Run # 11
Symbol O
Roughness 96 μ in. rms.

FIGURE 25

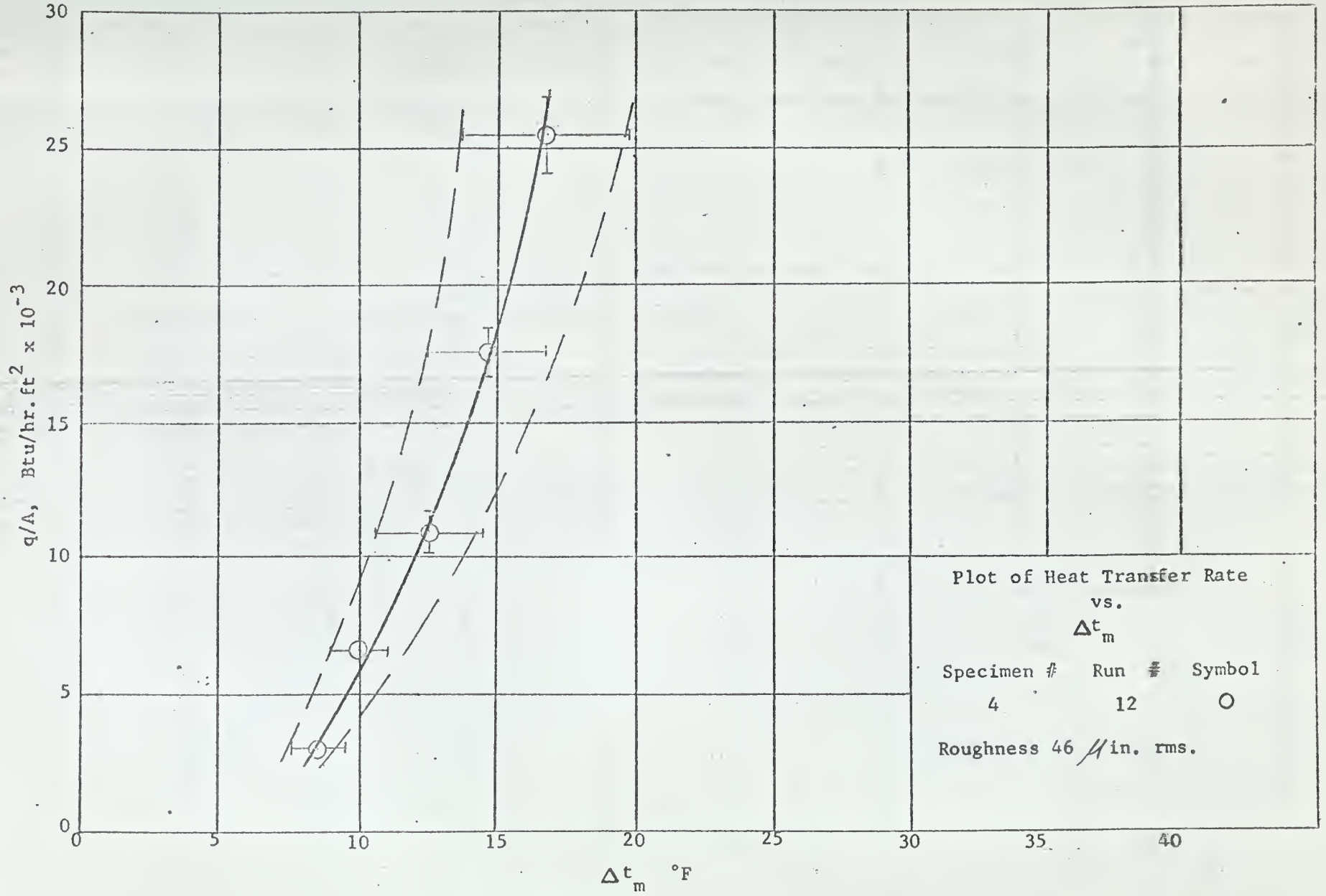
30
25
20
15
10
5
0
q/A, Btu/hr.ft^2 x 10^{-3}
0
5
10
15
20
25
30
35
40
Δt_m °F
Plot of Heat Transfer Rate
vs.
Δt_m
Specimen # Run # Symbol
4 12 O
Roughness 46 μin. rms.

FIGURE 26

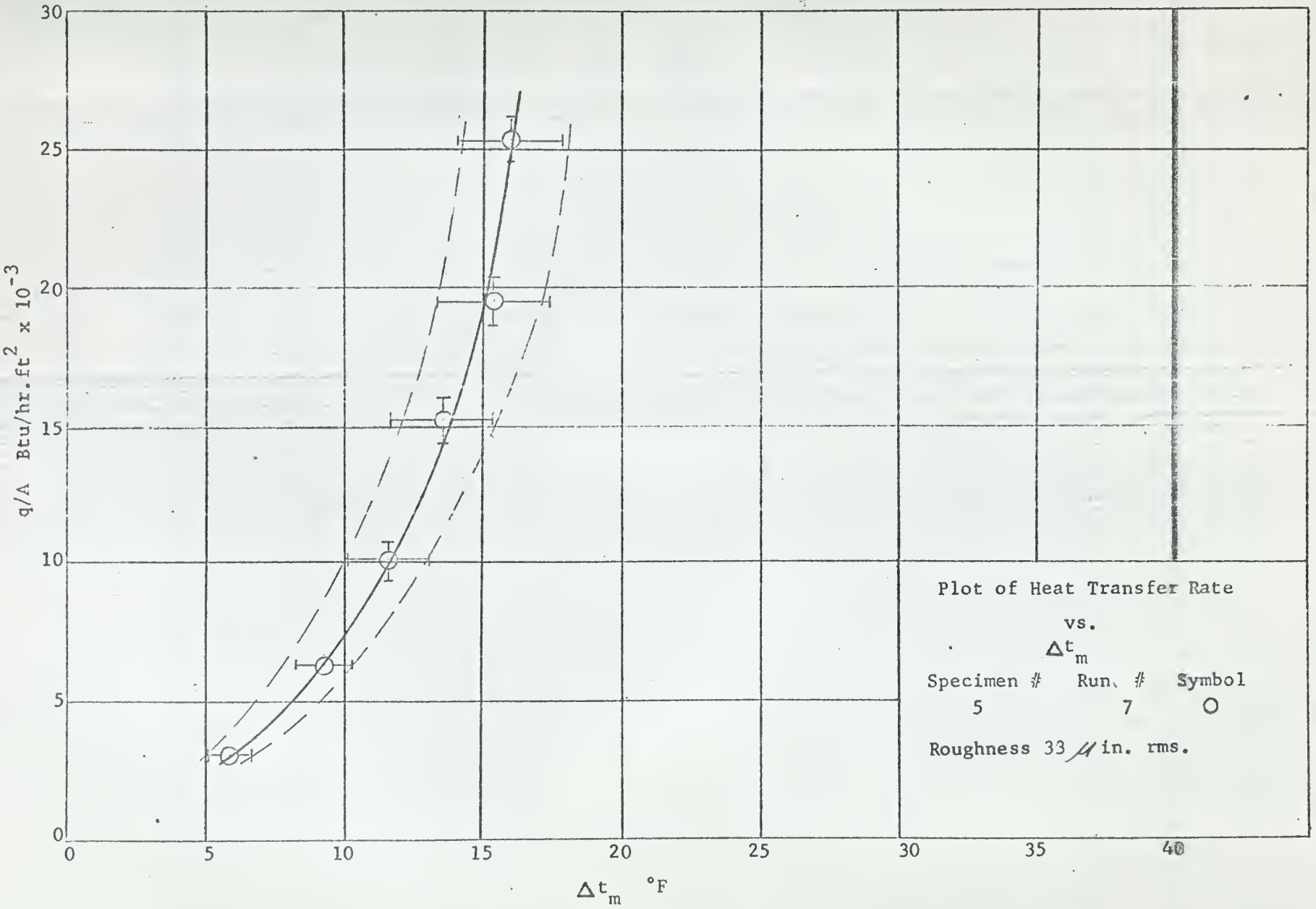
30
25
20
15
10
5
0
q/A Btu/hr.ft^2 x 10^{-3}
0
5
10
15
20
25
30
35
40
Δt_m °F
Plot of Heat Transfer Rate
vs.
Δt_m
Specimen # Run # Symbol
5 7 O
Roughness 33 µ in. rms.

FIGURE 27

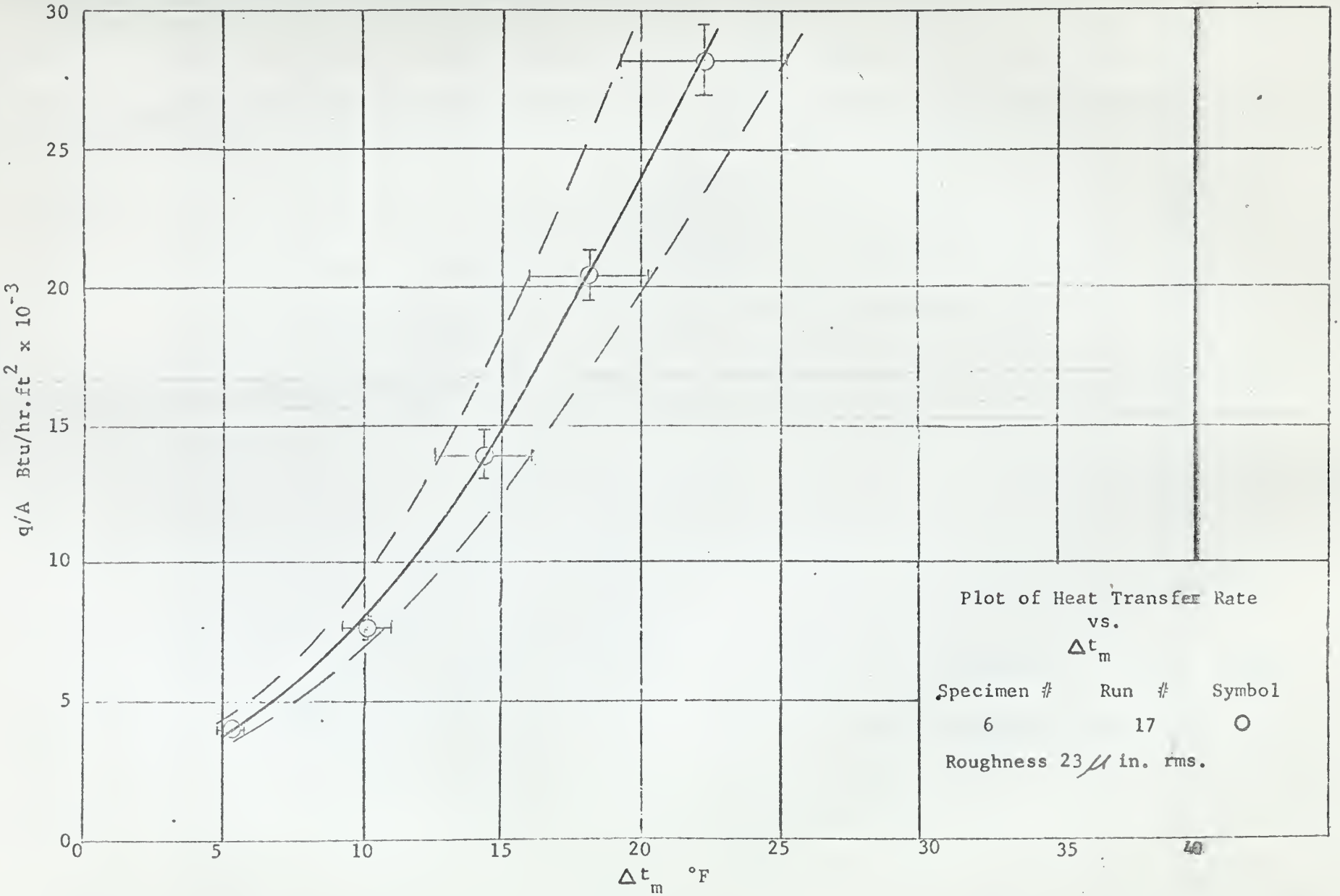
30
25
20
15
10
5
0
0
5
10
15
20
25
30
35
40
q/A Btu/hr.ft^2 x 10^{-3}
Δt_m °F
Plot of Heat Transfer Rate
vs.
Δt_m
Specimen # Run # Symbol
6 17 O
Roughness 23 μ in. rms.

FIGURE 28

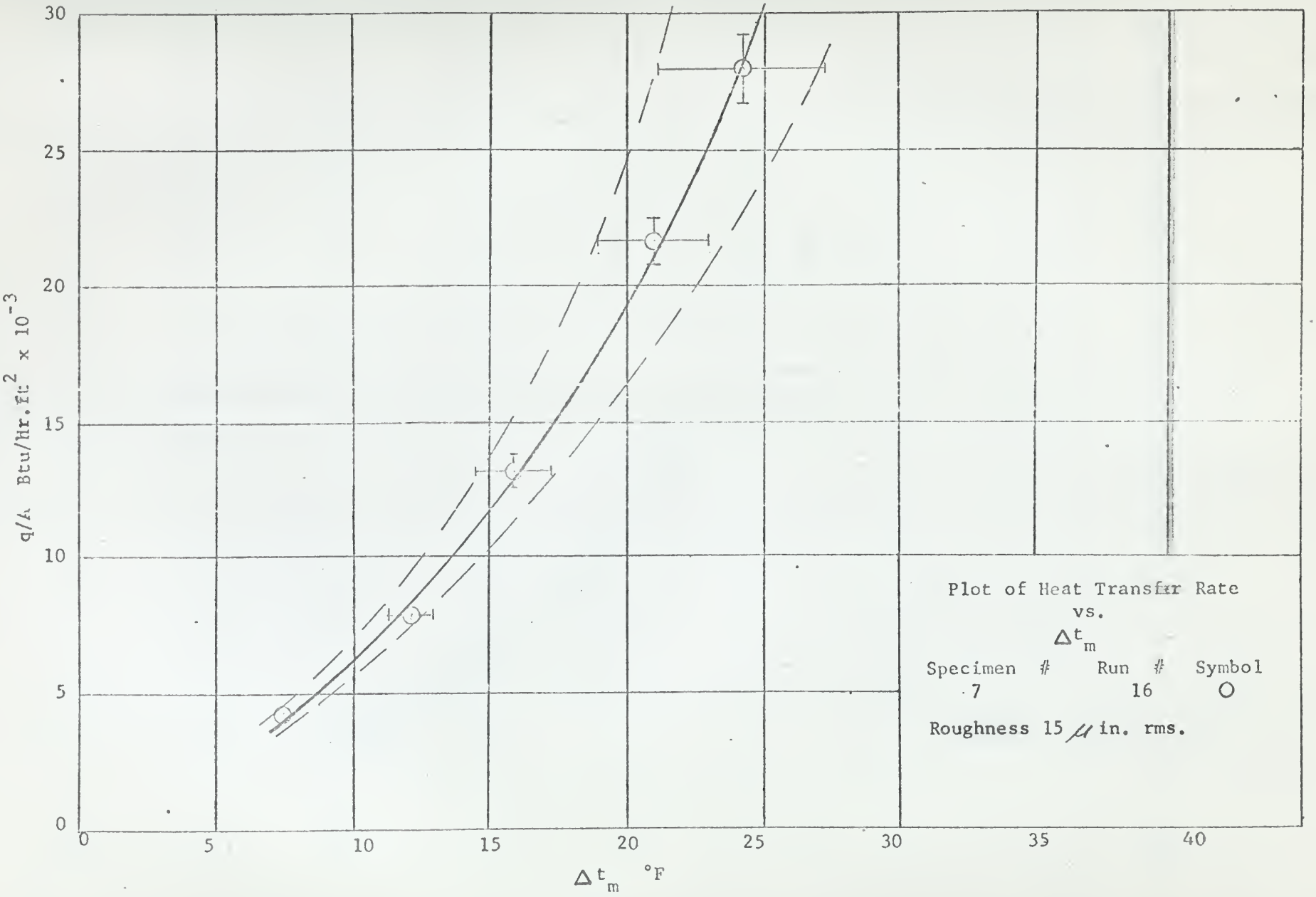
30
25
20
15
10
5
0
0
5
10
15
20
25
30
35
40
q/A Btu/Hr.Ft.^{2} x 10^{-3}
Δt_m °F
Plot of Heat Transfer Rate
vs.
Δt_m
Specimen # 7
Run # 16
Symbol O
Roughness 15 μ in. rms.

FIGURE 29

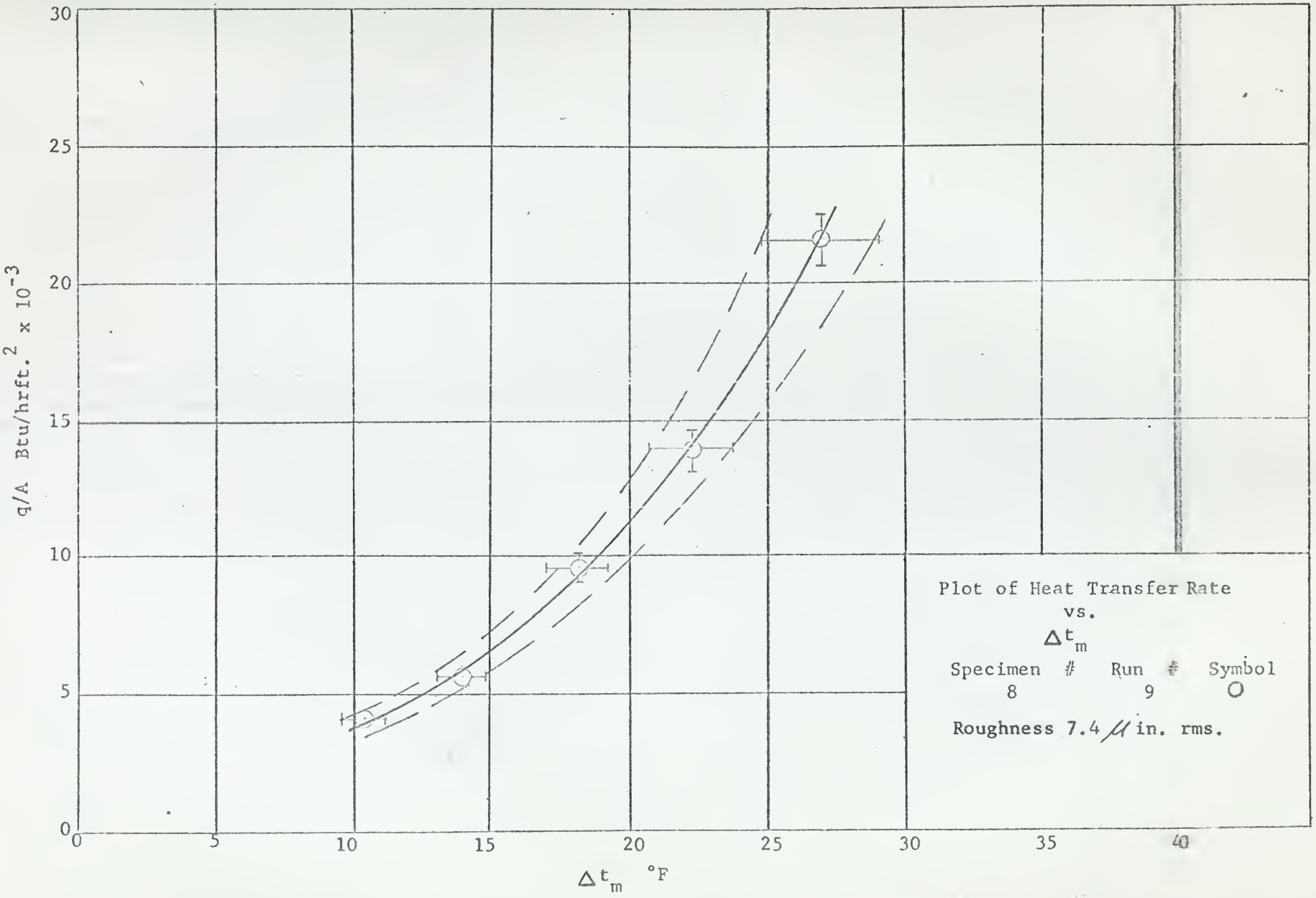
q/A Btu/hrft.^{2} x 10^{-3}
Δt_m °F
0
5
10
15
20
25
30
35
40
Plot of Heat Transfer Rate
vs.
Δt_m
Specimen # 8
Run # 9
Symbol O
Roughness 7.4 μ in. rms.

FIGURE 30

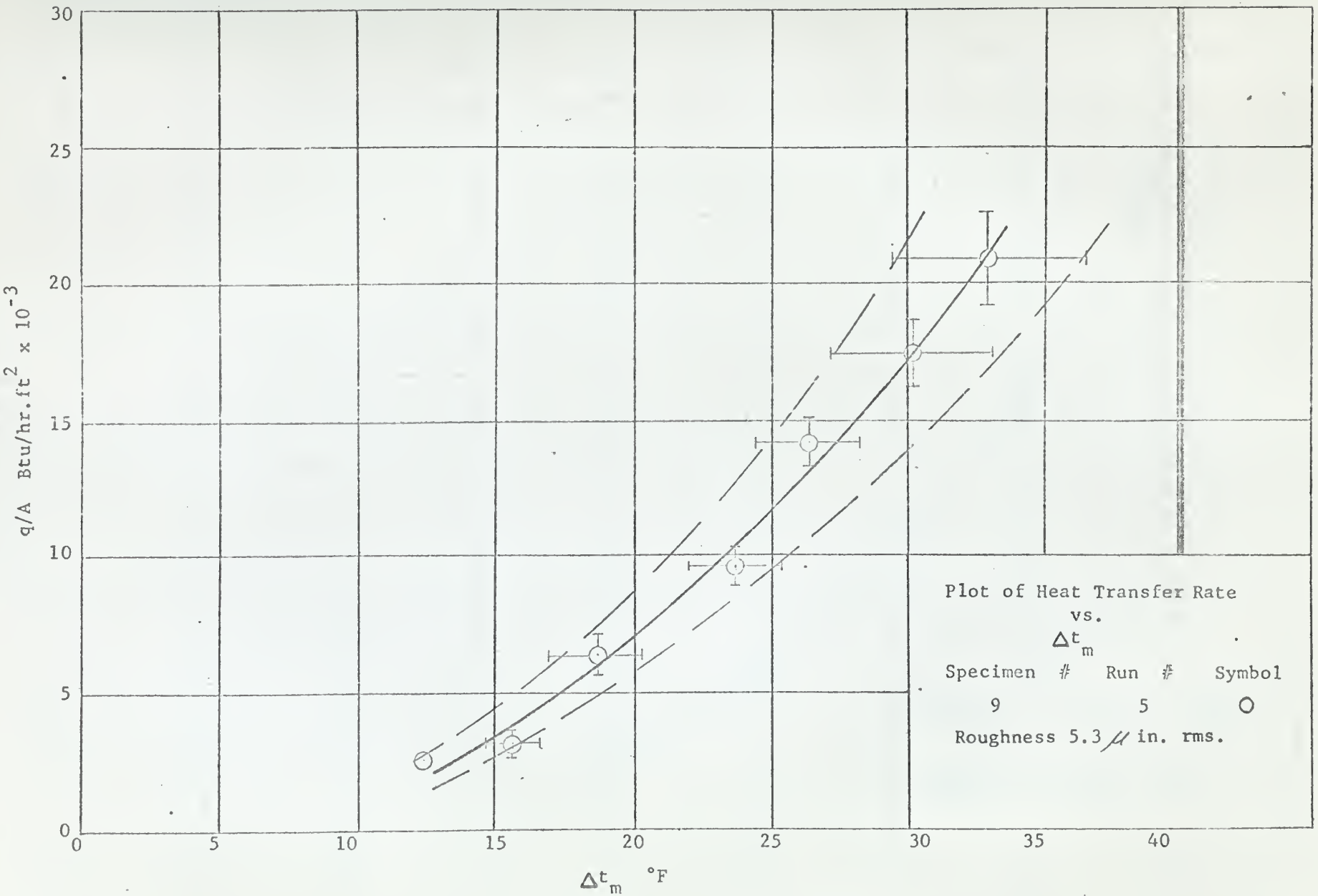
30
25
20
15
10
5
0
0
5
10
15
20
25
30
35
40
q/A Btu/hr.ft^2 x 10^{-3}
Δt_m °F
Plot of Heat Transfer Rate
vs.
Δt_m
Specimen # Run # Symbol
9 5 O
Roughness 5.3 μ in. rms.

FIGURE 31

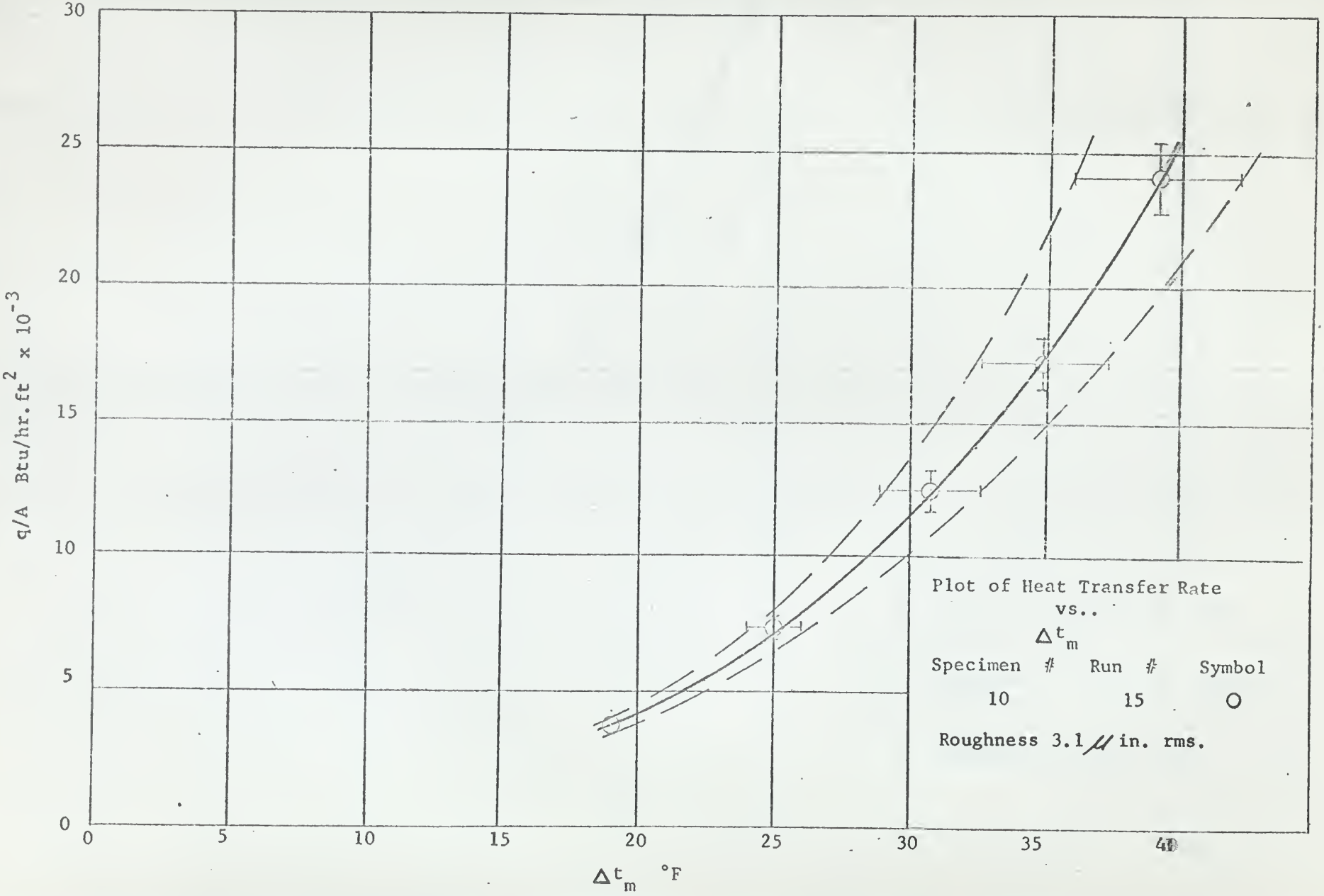
30
25
20
15
10
5
0
0
5
10
15
20
25
30
35
40
q/A Btu/hr.ft^2 x 10^{-3}
Δt_m °F
Plot of Heat Transfer Rate
vs..
Δt_m
Specimen # Run # Symbol
10 15 O
Roughness 3.1 μ in. rms.

FIGURE 32

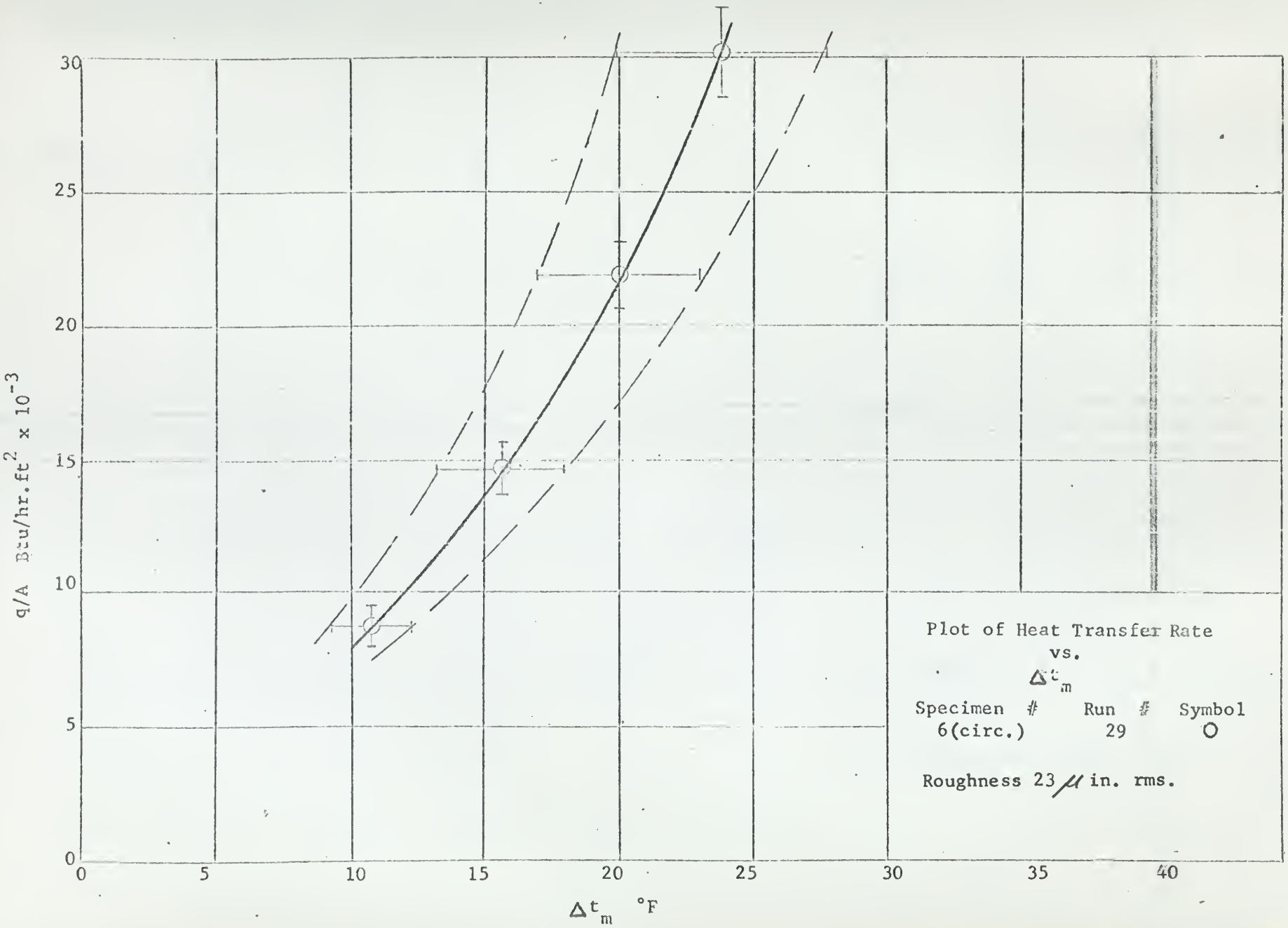
30
25
20
15
10
5
0
0
5
10
15
20
25
30
35
40
q/A Btu/hr.ft^2 x 10^{-3}
Δt_m °F
Plot of Heat Transfer Rate
vs.
Δt_m
Specimen # Run # Symbol
6(circ.) 29 O
Roughness 23 μ in. rms.

FIGURE 33

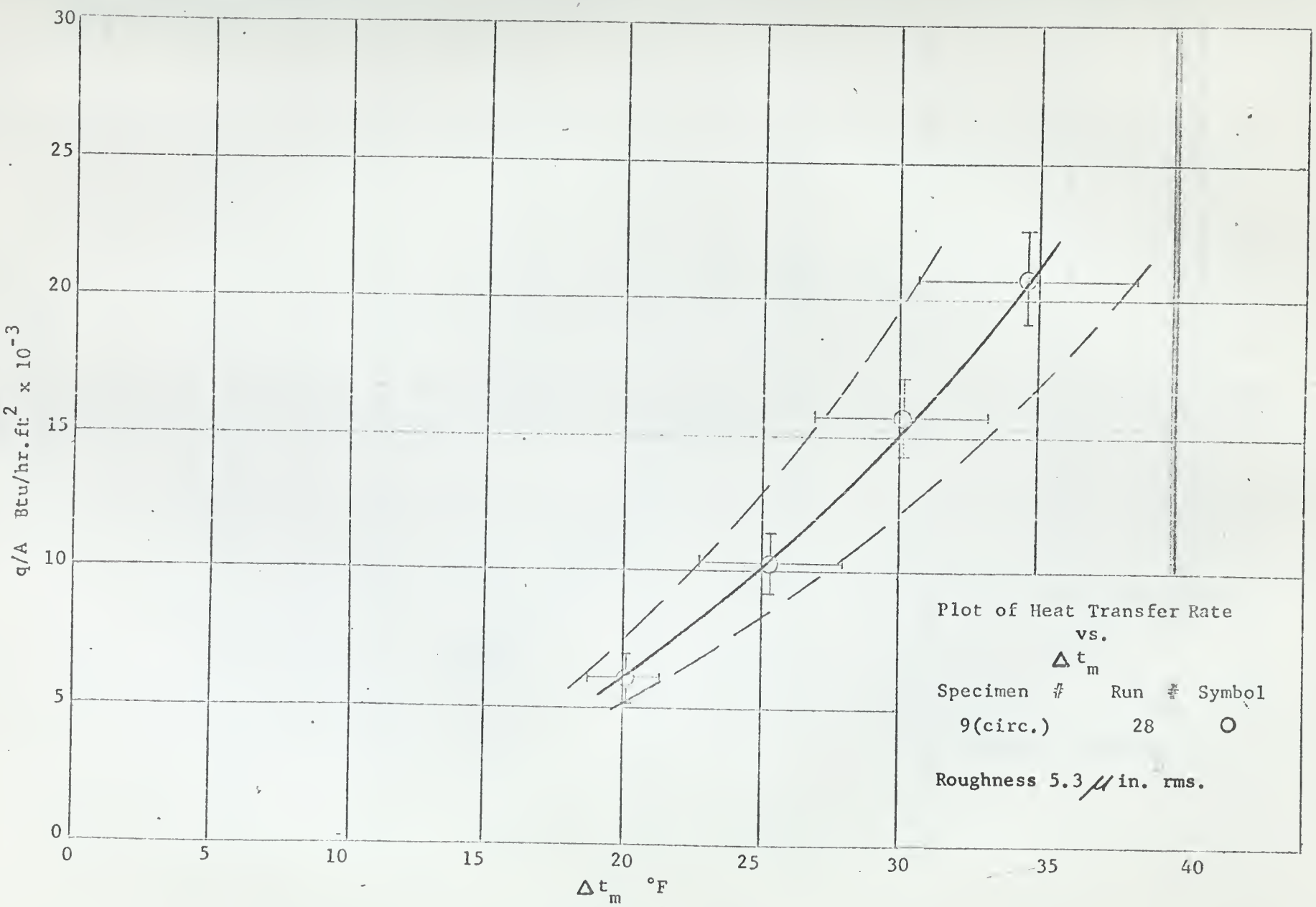
30
25
20
15
10
5
0
q/A Btu/hr.ft.^{2} x 10^{-3}
0
5
10
15
20
25
30
35
40
Δt_m °F
Plot of Heat Transfer Rate
vs.
Δt_m
Specimen # Run # Symbol
9(circ.) 28 O
Roughness 5.3 μ in. rms.

FIGURE 34

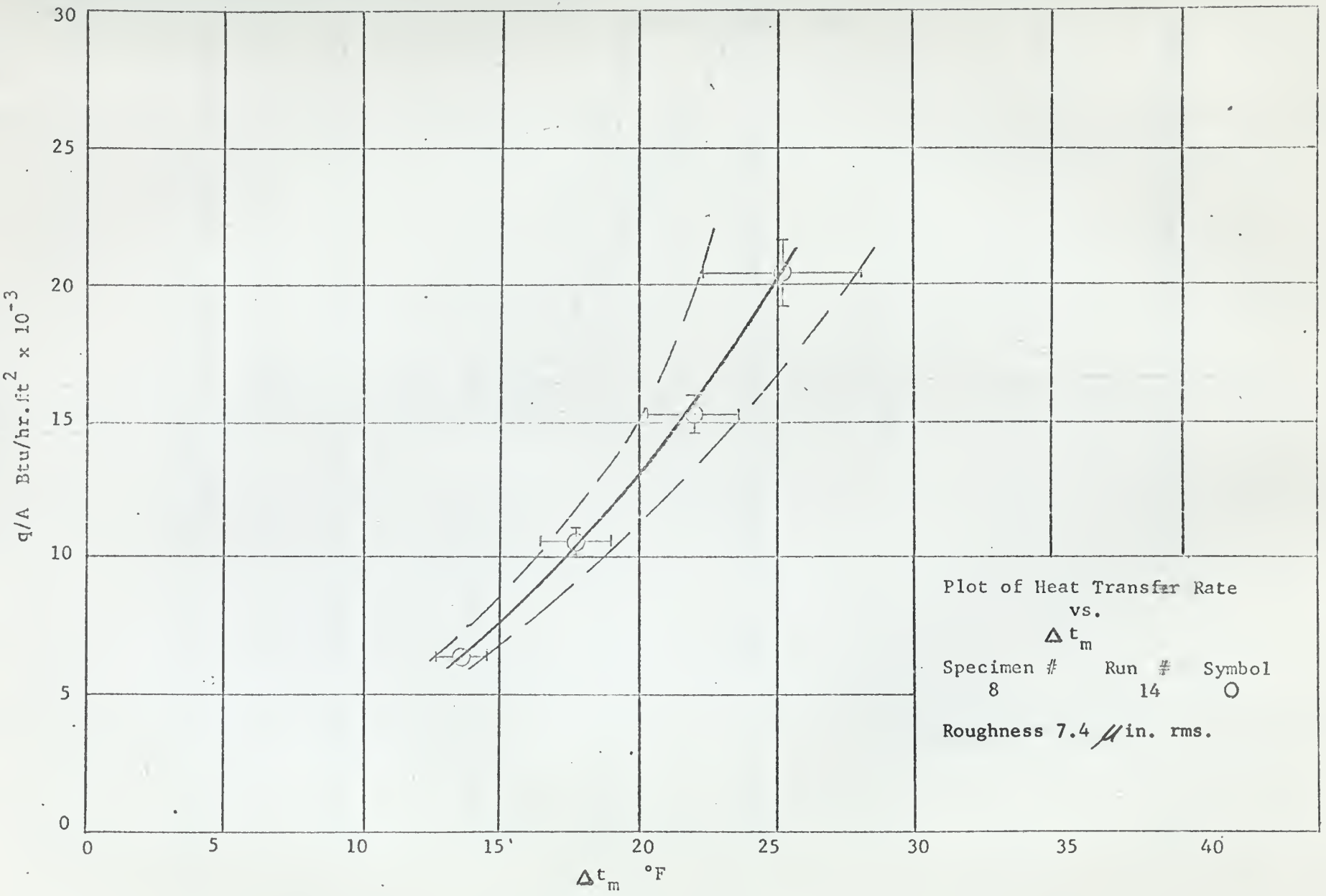
30
25
20
15
10
5
0
q/A Btu/hr.ft^2 x 10^{-3}
0
5
10
15
20
25
30
35
40
Δt_m °F
Plot of Heat Transfer Rate
vs.
Δt_m
Specimen # 8
Run # 14
Symbol O
Roughness 7.4 μin. rms.

FIGURE 35

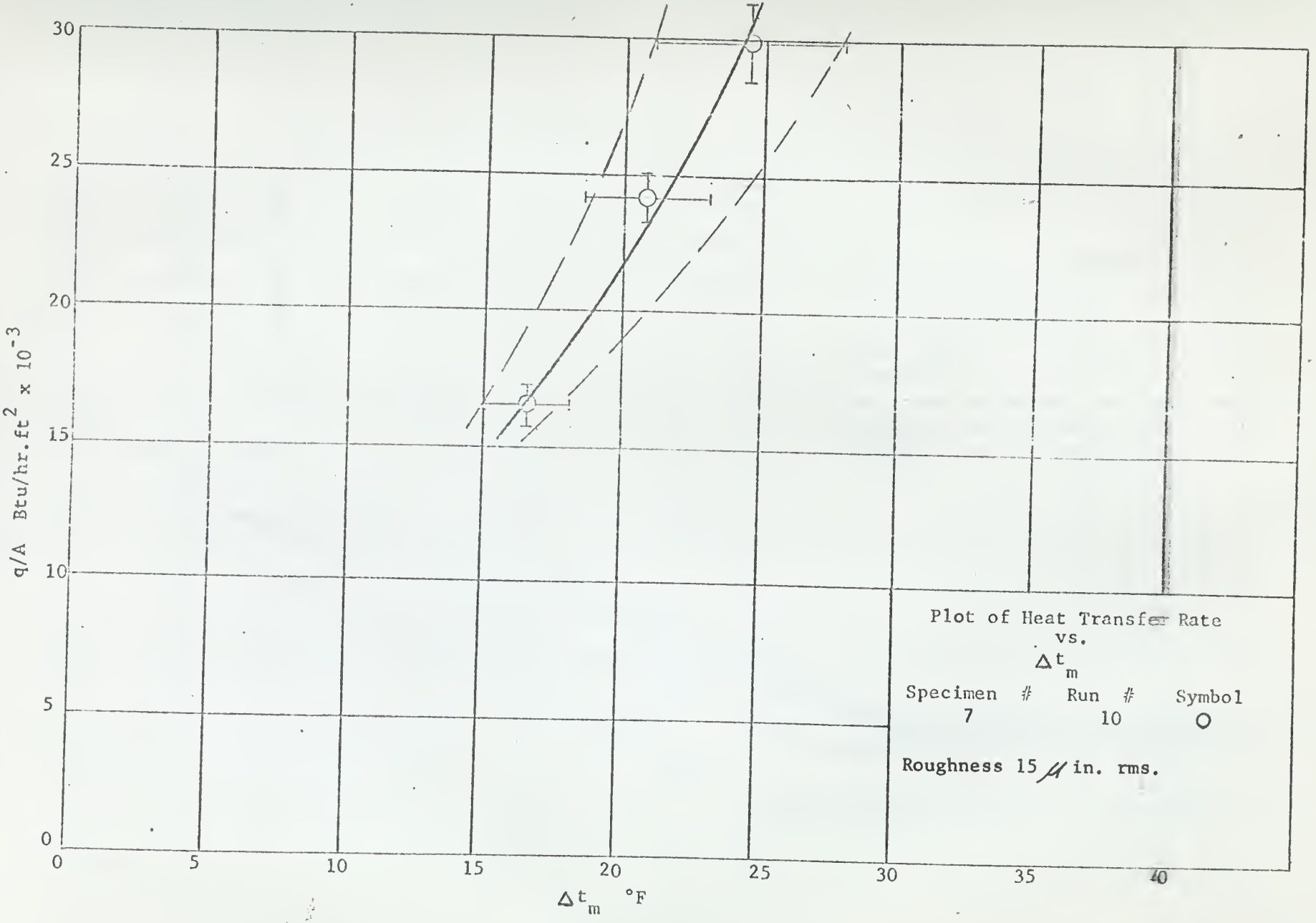
30
25
20
15
10
5
0
0
5
10
15
20
25
30
35
40
q/A Btu/hr.ft^2 x 10^{-3}
Δt_m °F
Plot of Heat Transfer Rate
vs.
Δt_m
Specimen # 7
Run # 10
Symbol O
Roughness 15 μ in. rms.

FIGURE 36

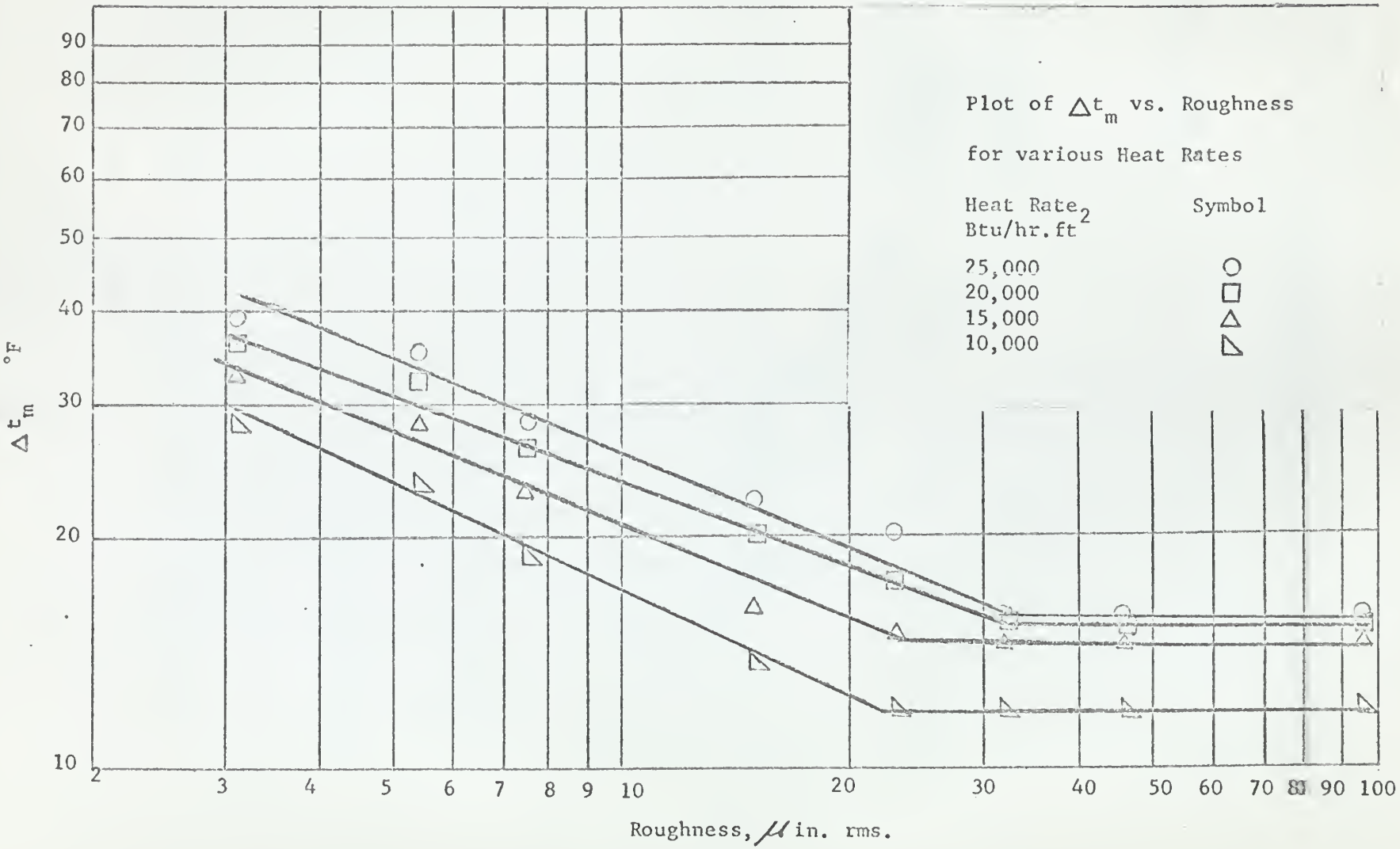
Plot of Δt_m vs. Roughness
for various Heat Rates
Heat Rate, Btu/hr.ft^2
Symbol
25,000
20,000
15,000
10,000
Δt_m °F
90
80
70
60
50
40
30
20
10
2
3
4
5
6
7
8
9
10
20
30
40
50
60
70
80
90
100
Roughness, μ in. rms.

FIGURE 37

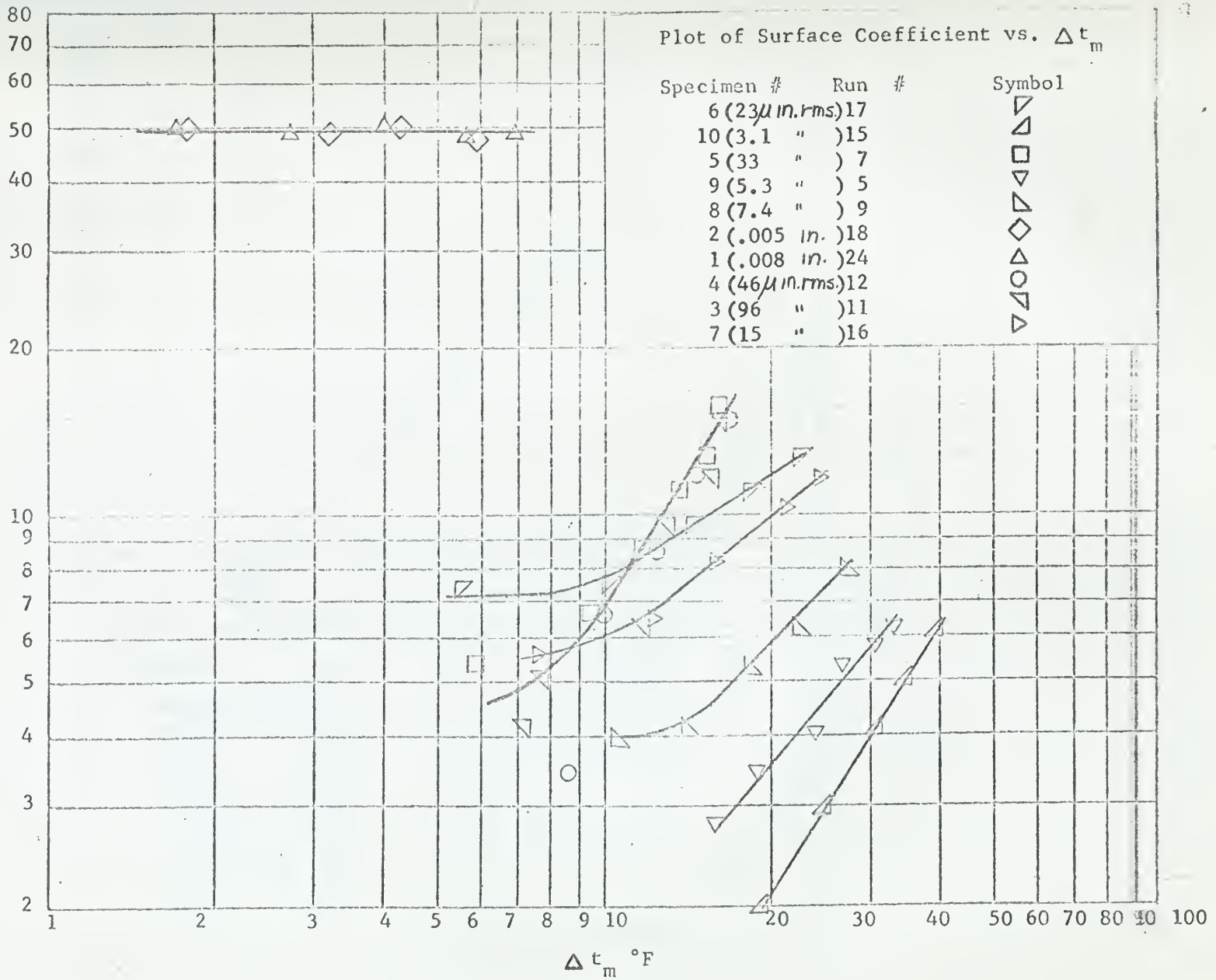
Plot of Surface Coefficient vs. Δt_m
Specimen # Run # Symbol
6 (23μ in. rms.) 17
10 (3.1 ") 15
5 (33 ") 7
9 (5.3 ") 5
8 (7.4 ") 9
2 (.005 in.) 18
1 (.008 in.) 24
4 (46μ in. rms.) 12
3 (96 ") 11
7 (15 ") 16
h, Btu/hr.ft^2°F x 10^{-2}
Δt_m °F
80
70
60
50
40
30
20
10
9
8
7
6
5
4
3
2
1
2
3
4
5
6
7
8
9
10
20
30
40
50
60
70
80
90
100

FIGURE 38

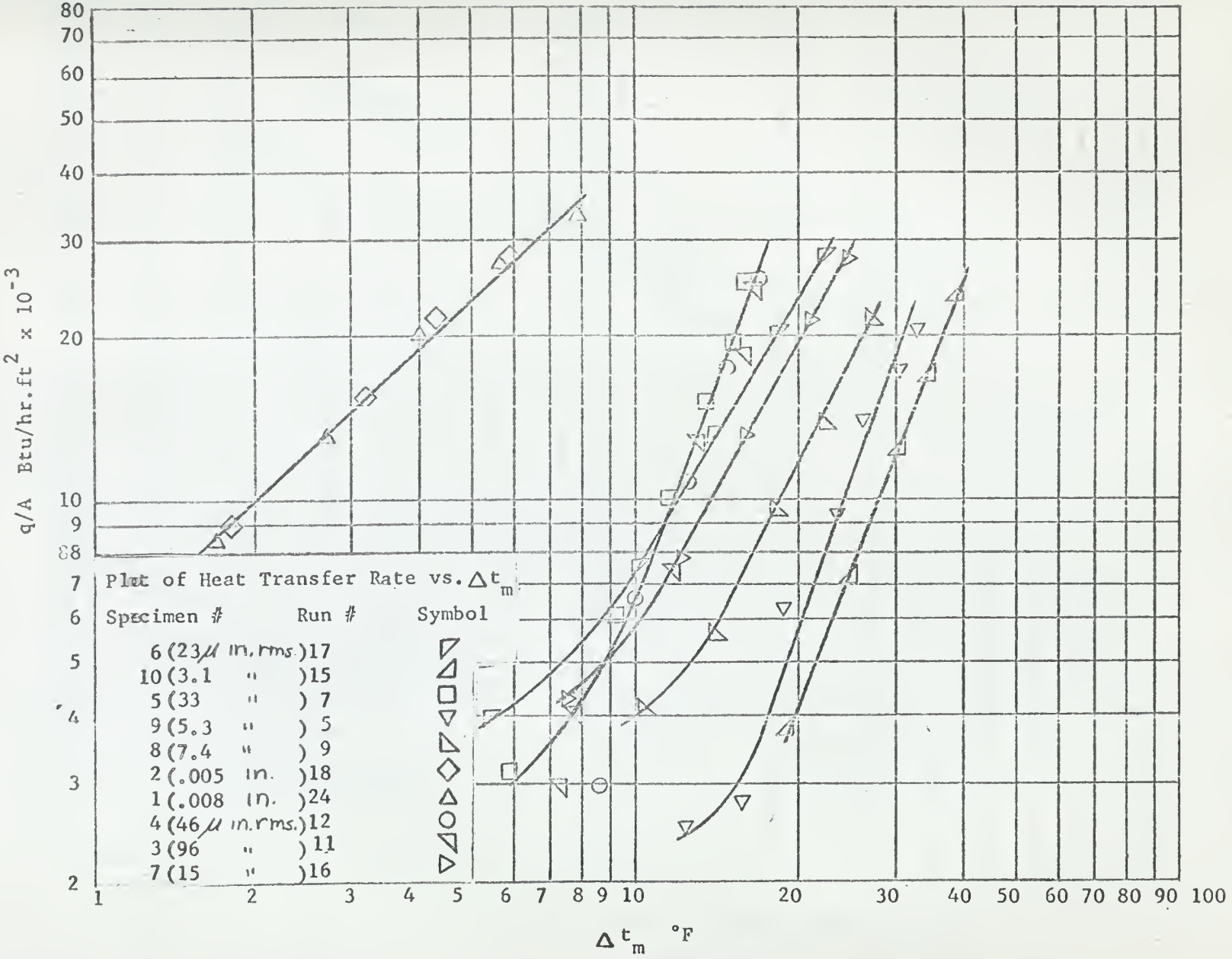
q/A Btu/hr.ft^2 x 10^{-3}
80
70
60
50
40
30
20
10
9
8
7
6
5
4
3
2
1
2
3
4
5
6
7
8
9
10
20
30
40
50
60
70
80
90
100
Δt_m °F
Plot of Heat Transfer Rate vs. Δt_m
Specimen # Run # Symbol
6 (23 μ in. rms.) 17
10 (3.1 ") 15
5 (33 ") 7
9 (5.3 ") 5
8 (7.4 ") 9
2 (.005 in.) 18
1 (.008 in.) 24
4 (46 μ in. rms.) 12
3 (96 ") 11
7 (15 ") 16

FIGURE 39

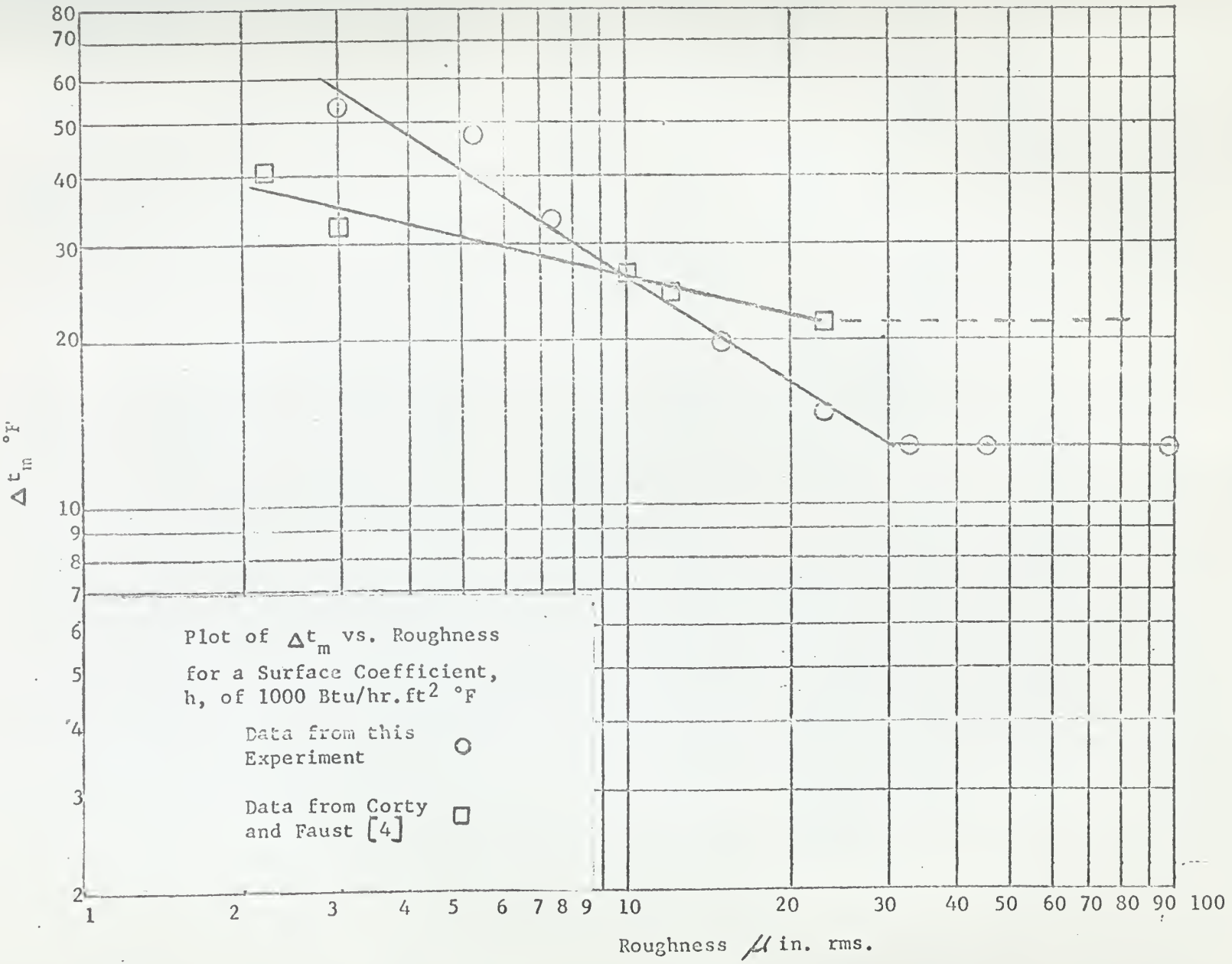
80
70
60
50
40
30
20
10
9
8
7
6
5
4
3
2
Δt_m °F
1
2
3
4
5
6
7
8
9
10
20
30
40
50
60
70
80
90
100
Roughness μ in. rms.
Plot of Δt_m vs. Roughness
for a Surface Coefficient,
h, of 1000 Btu/hr.ft^2 °F
Data from this Experiment
Data from Corty and Faust [4]

FIGURE 40

APPENDIX B

SAMPLE CALCULATIONS

These sample calculations are for Run #7. The data for this run is shown in Table II, Sampe Data Sheet.

$$\bar{t}_A = \frac{t_1 + t_6 + t_3 + t_4}{4} = \frac{243.3 + 245.7 + 246.0 + 242.7}{4} = 244.4\,^{\circ}F$$

$$\bar{t}_B = \frac{t_2 + t_5}{2} = \frac{308.0 + 302.5}{2} = 305.3\,^{\circ}F$$

$$\left(\frac{\Delta \bar{t}}{\Delta x}\right)_{A-B} = \frac{\bar{t}_B - \bar{t}_A}{\Delta x)_{A-B}} = \frac{305.3 - 244.4}{.270} = \frac{60.9}{.270} = 225.0\,^{\circ}F/in.$$

$$\bar{t}_s = \bar{t}_A - \Delta x)_{A-S}\left(\frac{\Delta \bar{t}}{\Delta x}\right)_{A-B} = 244.4 - 0.073(225.0) = 228.0\,^{\circ}F$$

$$\Delta t_m = \bar{t}_s - t_w = 228.0 - 212.0 = 16.0\,^{\circ}F$$

where: $\bar{t}_A$ = average temperature at level A in the specimen

$\bar{t}_B$ = average temperature at level B in the specimen

$t_{1,2, \text{ etc.}}$ = temperature at thermocouple locations shown in Fig. 9.

$\bar{t}_s$ = average temperature of heating surface

t_w = temperature of distilled water

using K = 9.4 Btu/hr ft°F for type 304 stainless steel as found in the Metals Handbook [19] .

$$q/A = K\,\frac{\Delta t}{\Delta x} = 9.4\ (225.0)\ (12) = 25400 \text{ Btu/hr ft}^2$$

$\bar{t}_A = 244.4 \pm 1.7°F$, $\bar{t}_B = 305.3 \pm 2.8°F$

$\Delta\bar{t} = \bar{t}_B - \bar{t}_A$

Let the uncertainty in

$$\Delta\bar{t} = w$$
$$\bar{t}_A = \Delta\bar{t}_A$$
$$\bar{t}_B = \Delta\bar{t}_B$$
$$\bar{t}_s = \Delta\bar{t}_s$$

therefore:

$$w = \pm\sqrt{(\Delta\bar{t}_A)^2 + (\Delta\bar{t}_B)^2} = \pm\sqrt{(1.7)^2 + (2.8)^2}$$
$$= \pm\sqrt{2.89 + 7.84} = \pm 3.28°F$$

$$\bar{t}_s = \bar{t}_A - \Delta X)_{A-S}\left(\frac{\Delta\bar{t}}{\Delta X}\right)_{A-B}$$

Since the uncertainty in ΔX is negligible in comparison with w.

$$\Delta t_s = \pm\sqrt{(\Delta\bar{t}_A)^2 + \left[\frac{\Delta X)_{A-S}\, w}{\Delta X)_{A-B}}\right]^2}$$

$$= \pm\sqrt{(1.7)^2 + \left[\left(\frac{.073}{.270}\right)3.28\right]^2} = \pm\sqrt{2.89 + .78}$$

$$= \pm 1.92 \simeq \pm 1.9°F$$

$\Delta t_m = \bar{t}_s - t_w$ However the uncertainty in t_w is negligible in comparison with $\bar{t}_s$.

therefore:

$$\Delta t_m = (\bar{t}_s \pm \Delta\bar{t}_s) - t_w = (228.0 \pm 1.9) - 212.0$$
$$= 16.0 \pm 1.9°F$$

$$q/A = \frac{k \Delta t}{\Delta x}$$ Let the uncertainty in $q/A = \Delta(q/A)$

$$\frac{\Delta(q/A)}{q/A} = \frac{w}{\Delta t} \; ; \quad \Delta(q/A) = q/A\left(\frac{w}{\Delta t}\right) = 25400\left(\frac{3.28}{60.9}\right) = \pm 1370 \frac{Btu}{hr.\,ft^2}$$

CALCULATION OF THE TIP TEMPERATURE FOR SURFACE IRREGULARITIES

$$\frac{T - T_\infty}{T_s - T_\infty} = I_o\left(\frac{2B\sqrt{x}}{2B\sqrt{L}}\right) ; \quad B = \sqrt{\frac{2L\bar{h}}{kt}}$$

where T_∞ = bulk temperature of water = 212°F

T_s = temperature at the base of the irregularities = 218.1°F

T = temperature at the point of interest on the irregularities

x = distance from tip to point of interest, ($x = 0$ at tip)

L = height of irregularities = 0.005 inches

$\bar{h}$ = average heat transfer coefficient = 1000 Btu/hr ft^2°F

k = thermal conductivity = 9.4 Btu/hr ft^2°F/ft

t = thickness of irregularities at base = 2/3 L

$\bar{h}$ was assumed equal to the above value as this is the same order of magnitude as that found in the results of this experiment.

Solving: $B = 13.6$

$2B\sqrt{L} = 0.55$

$I_o(2B\sqrt{L}) = 1.077$

$T = 217.7$°F

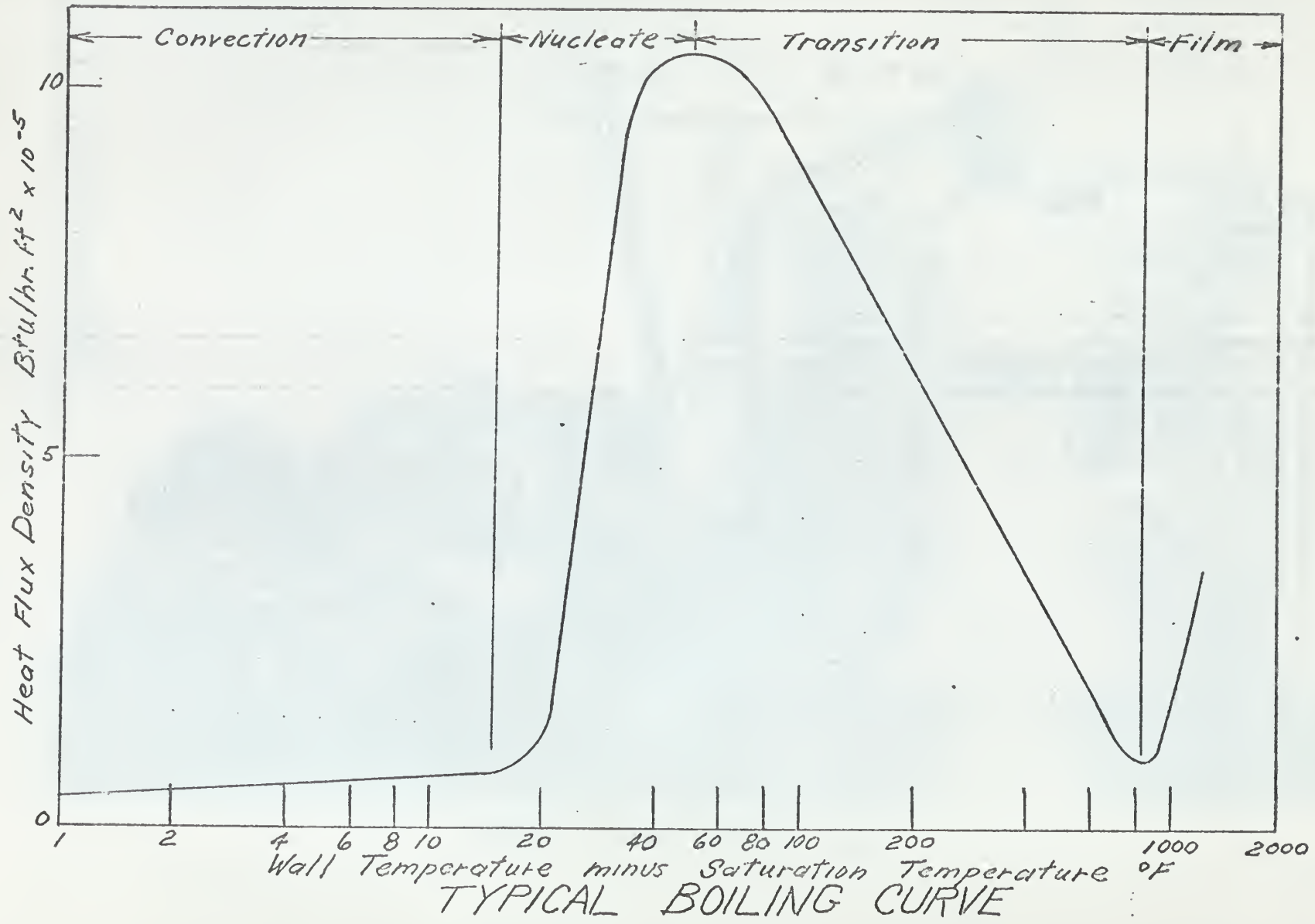
Convection
Nucleate
Transition
Film
Heat Flux Density B.t.u/hr. ft² x 10⁻⁵
10
5
0
1
2
4
6
8
10
20
40
60
80
100
200
1000
2000
Wall Temperature minus Saturation Temperature °F
TYPICAL BOILING CURVE

FIGURE 1

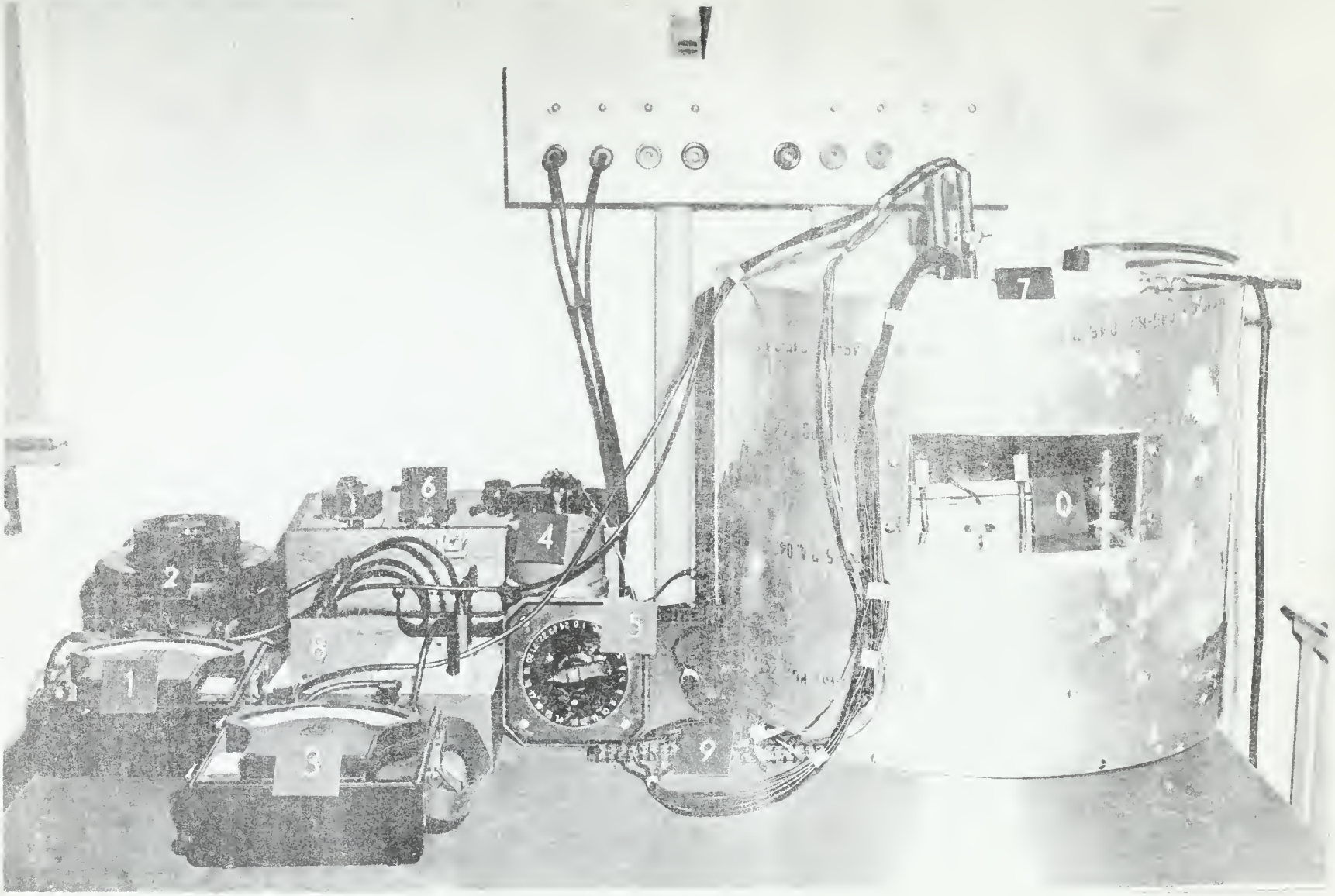

FIGURE 2 Overall Equipment Layout

FIGURE 2

EQUIPMENT IDENTIFICATION SYMBOLS

1	Alternating Current Voltmeter
2	Variac
3	Alternating Current Ammeter
4	Ice Bath
5	Thermocouple Switch
6	Thermocouple Potentiometer
7	Distilled Water Bath
8	Junction Box
9	Terminal Block
0	Mounting Block

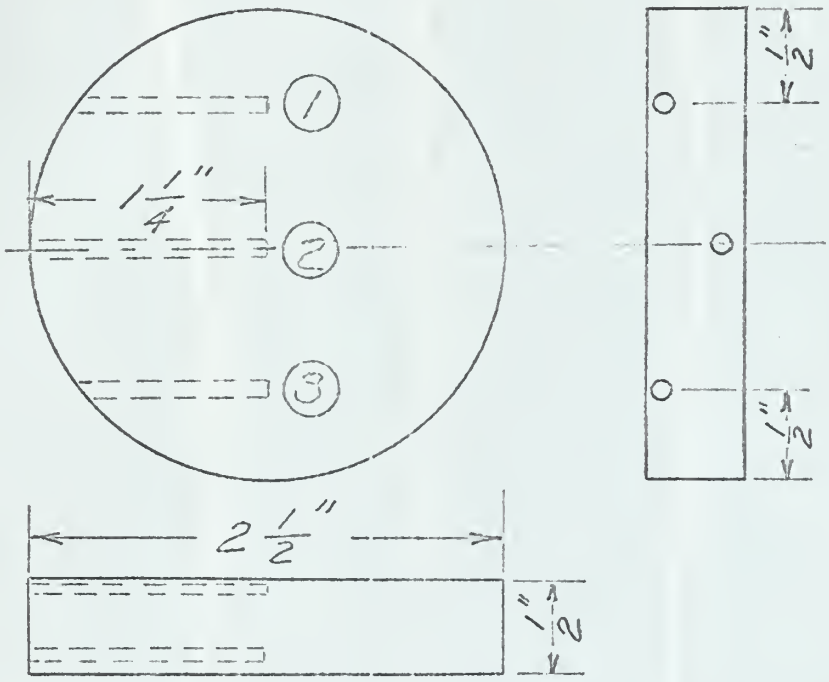

NOTES

1. ALL HOLES #49 DRILL
2. UPPER HOLES 1/16" BELOW SURFACE
3. LOWER HOLE 1/8" ABOVE SURFACE
4. NUMBERS IN CIRCLES ARE THERMOCOUPLE REFERENCE NUMBERS

TEST SPECIMEN AND THERMOCOUPLE SCHEDULE

FIGURE 3

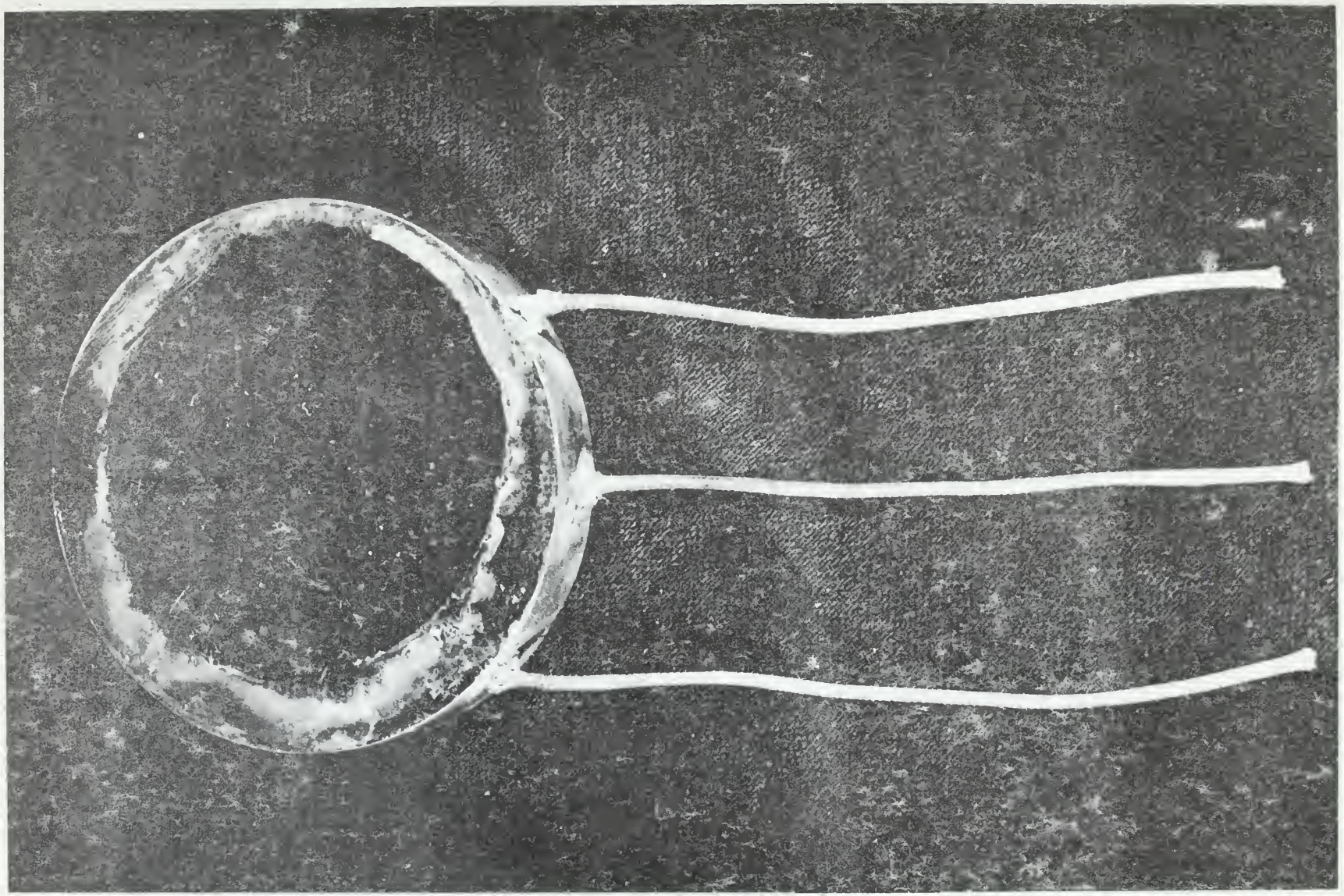

FIGURE 4 Circular Test Specimen

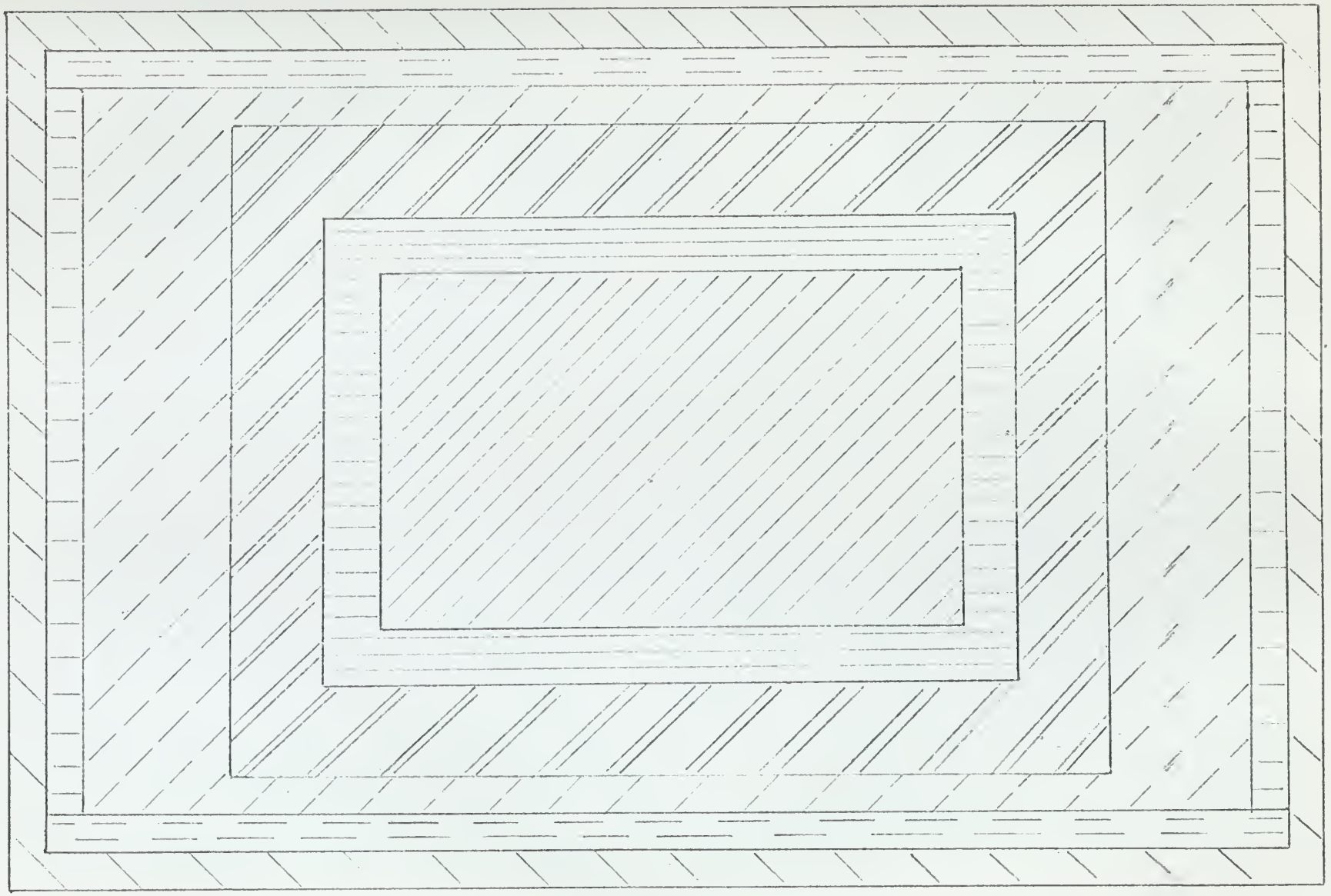

PLAN VIEW CROSS SECTION – MOUNTING BLOCK Scale 1:1

FIGURE 5

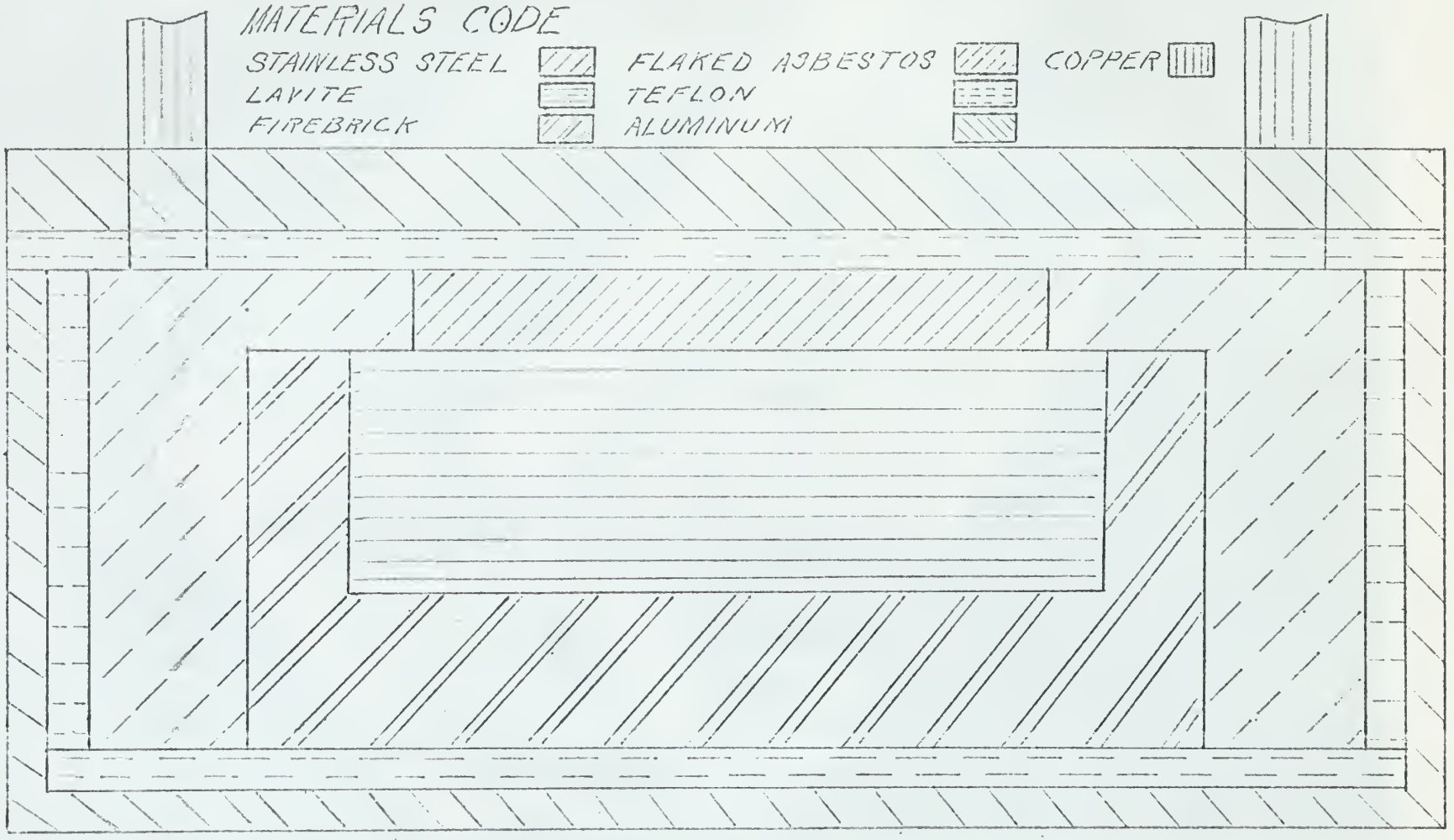

ELEVATION VIEW CROSS SECTION - MOUNTING BLOCK

Scale 1:1

FIGURE 6

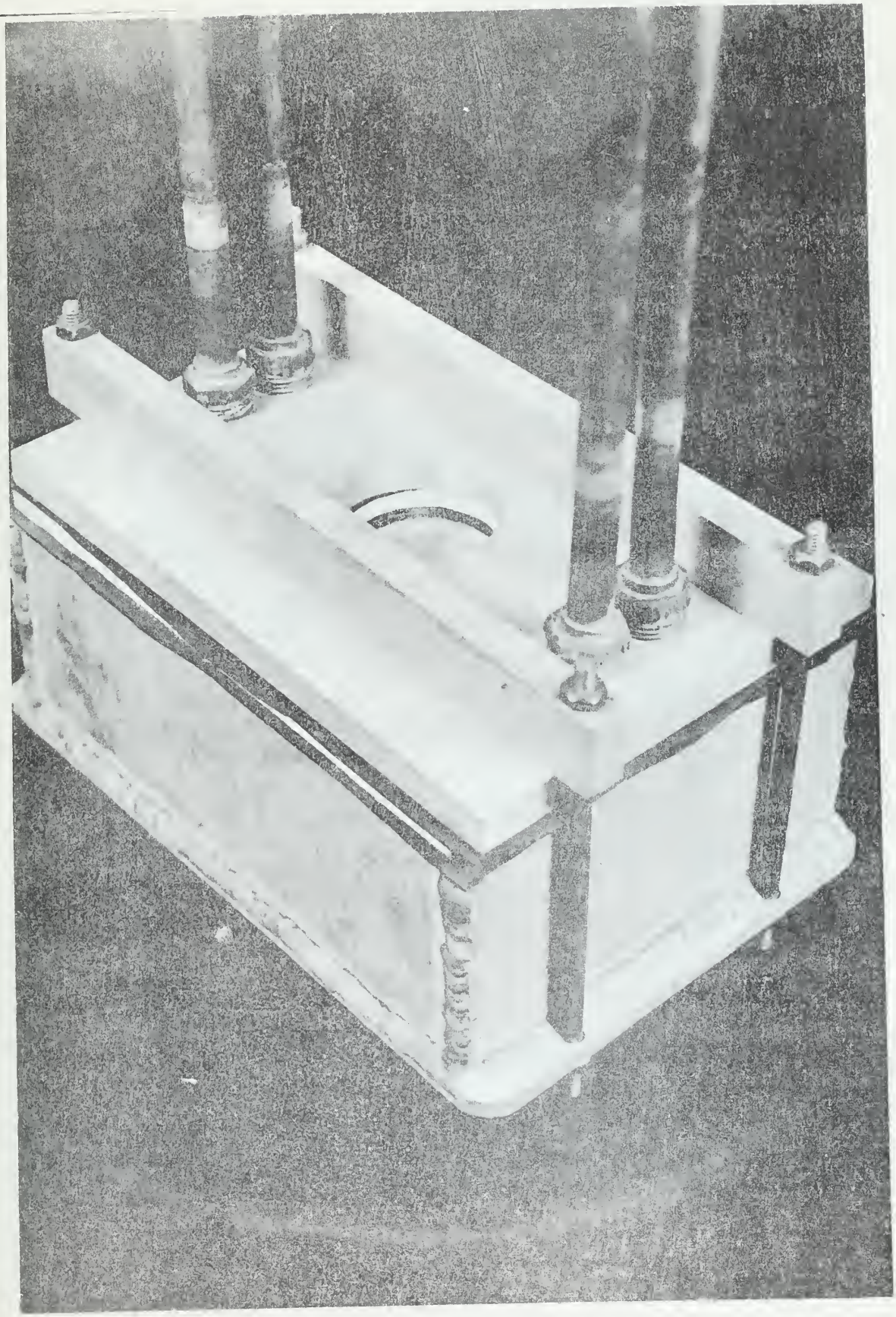

FIGURE 7 Specimen Mounting Block

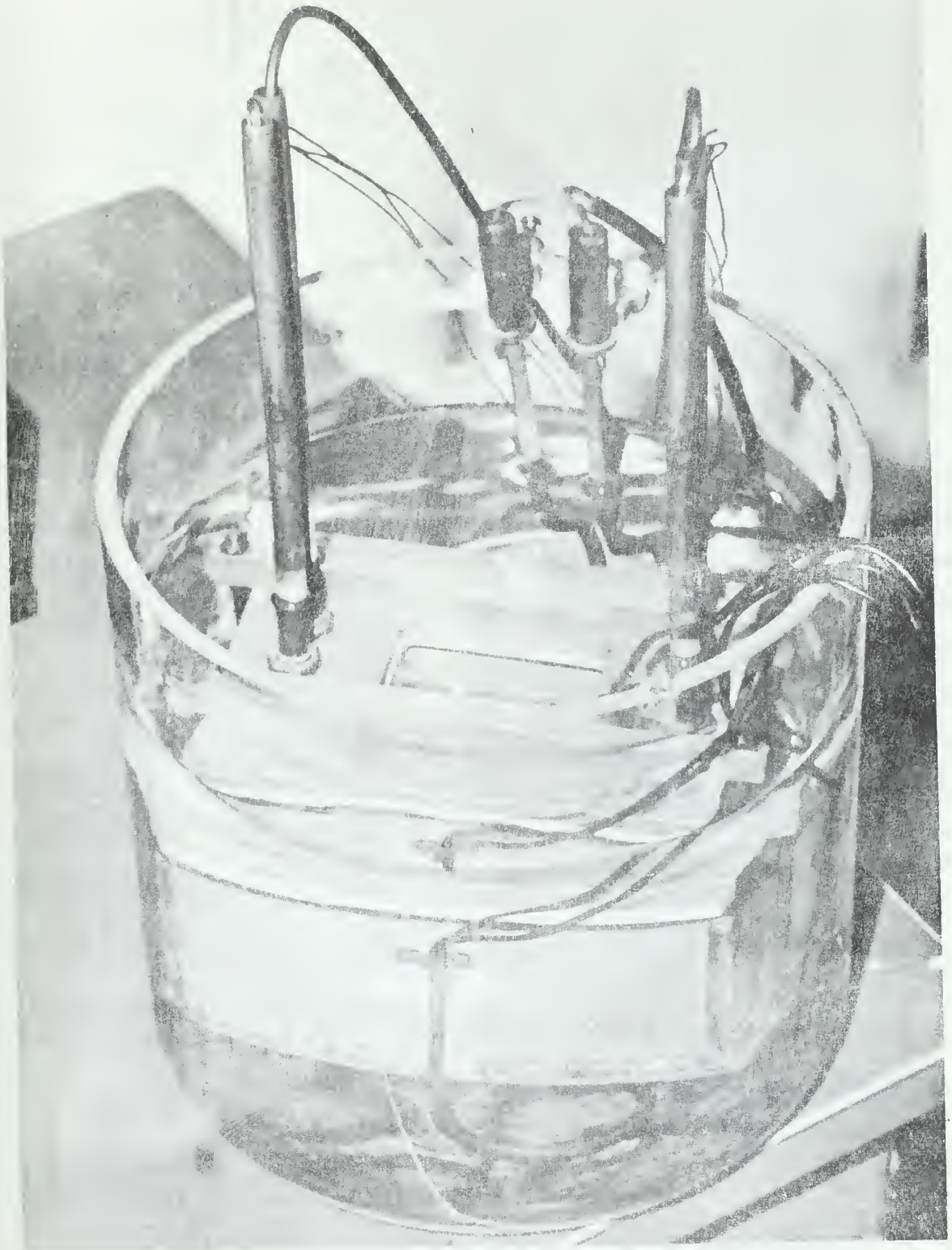

MATERIAL: 304 STAINLESS STEEL

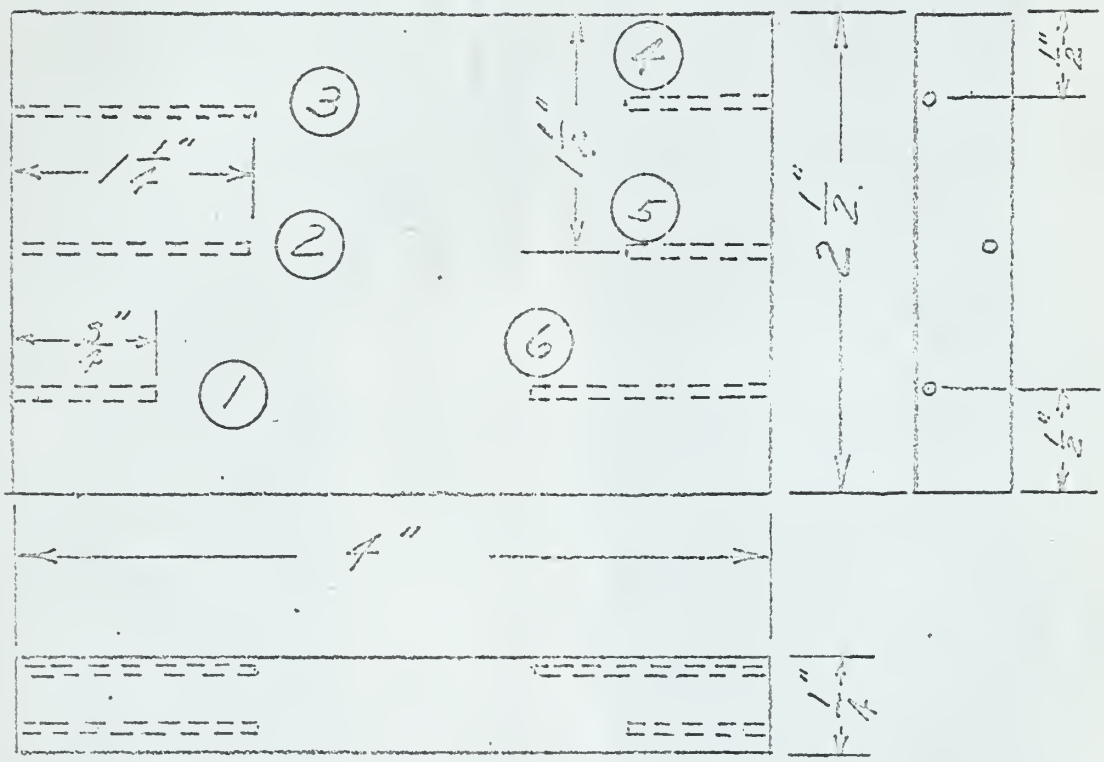

NOTES:

1. ALL HOLES #49 DRILL
2. DEPTH OF HOLES EITHER 1/4" OR 3/8"
3. UPPER HOLES 1/16" BELOW SURFACE
4. LOWER HOLES 1/8" ABOVE SURFACE
5. LARGE NUMBERS IN CIRCLES ARE REFERENCE NUMBERS FOR EASE IN IDENTIFYING TEMPERATURES

TEST SPECIMEN AND THERMOCOUPLE SCHEDULE

Figure 9

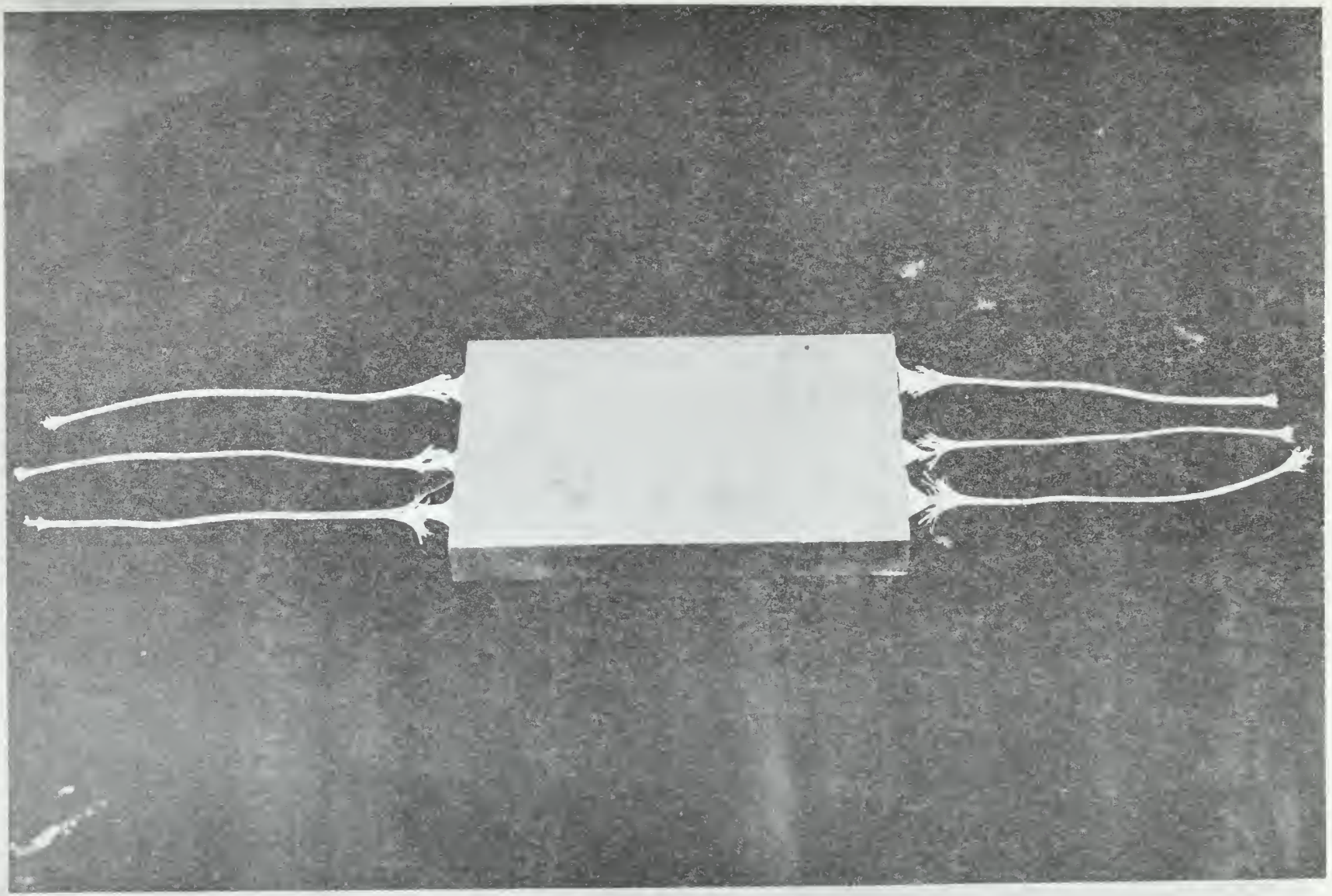

FIGURE 10 Rectangular Test Specimen

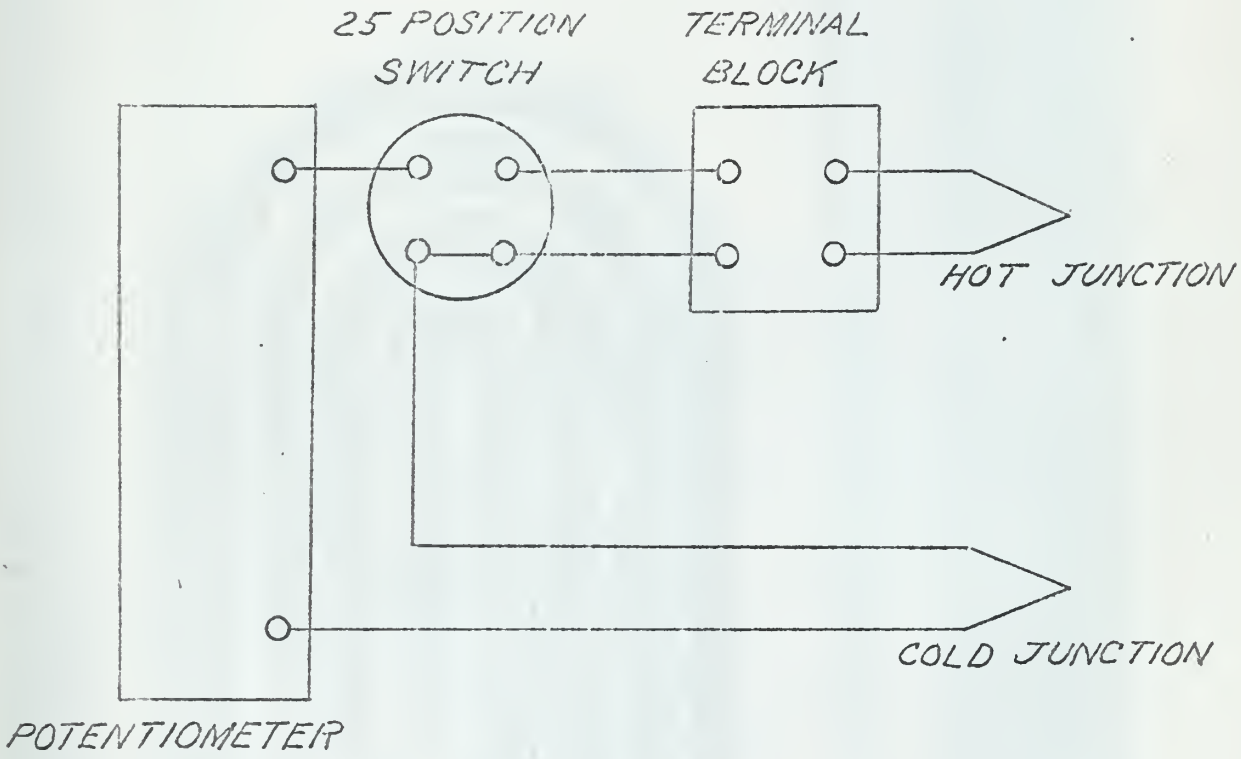

THERMOCOUPLE CIRCUIT DIAGRAM

FIGURE 11

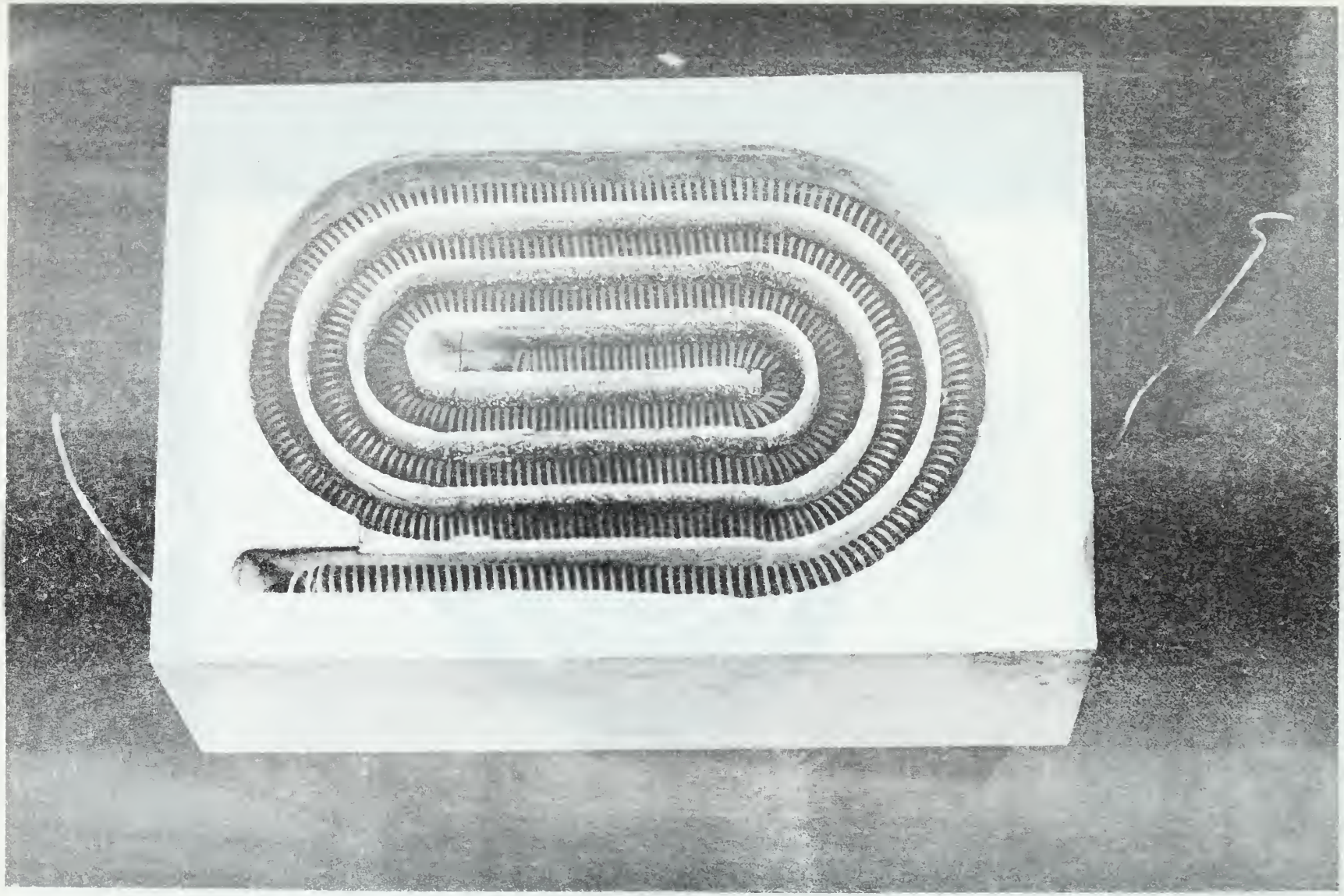

FIGURE 12 Rectangular Heating Coil

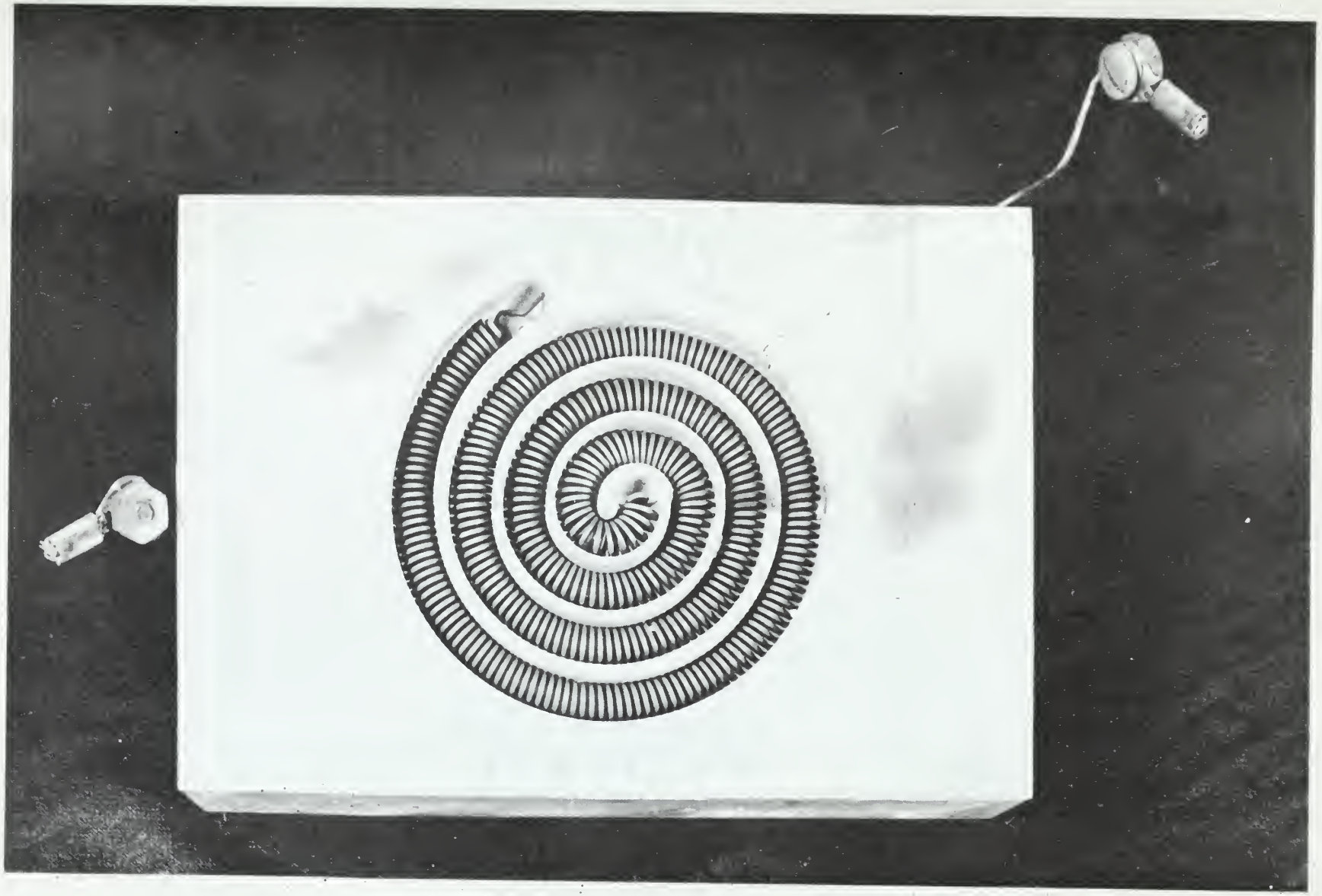

FIGURE 13 Circular Heating Coil

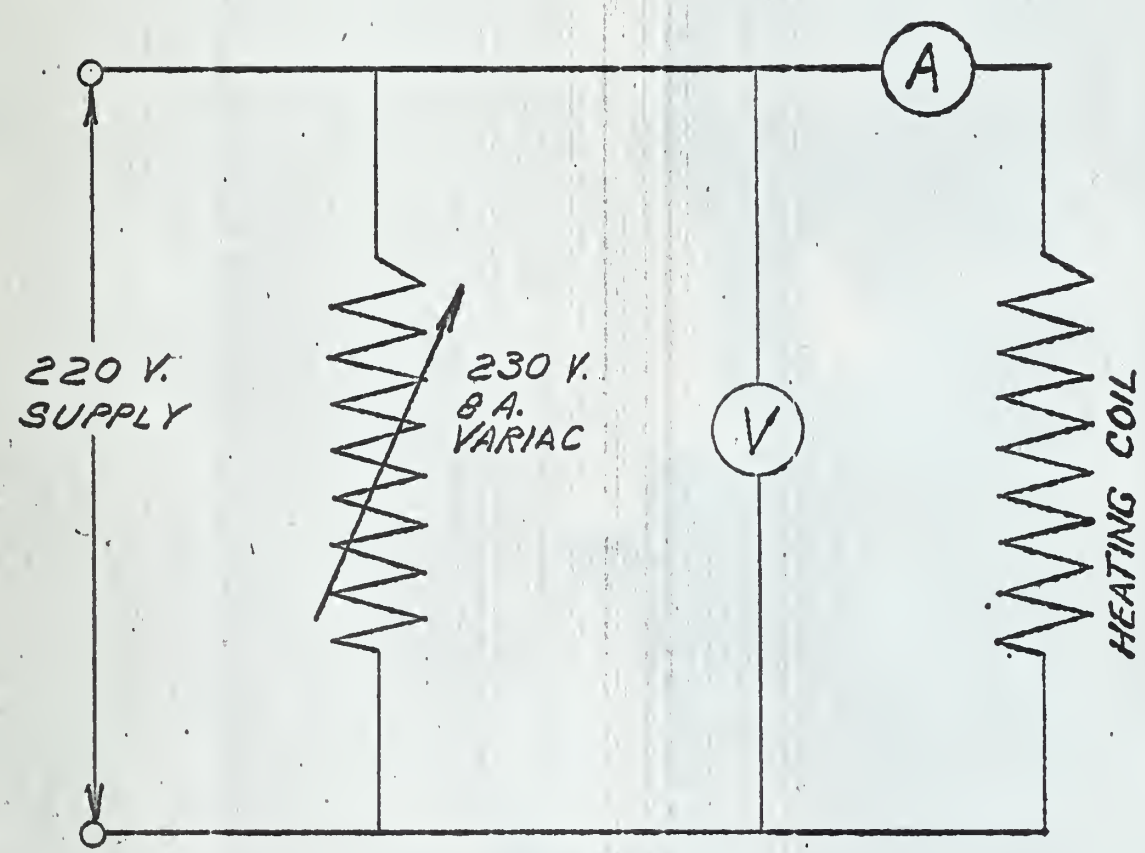

ELECTRICAL CIRCUIT DIAGRAM

FIGURE 14

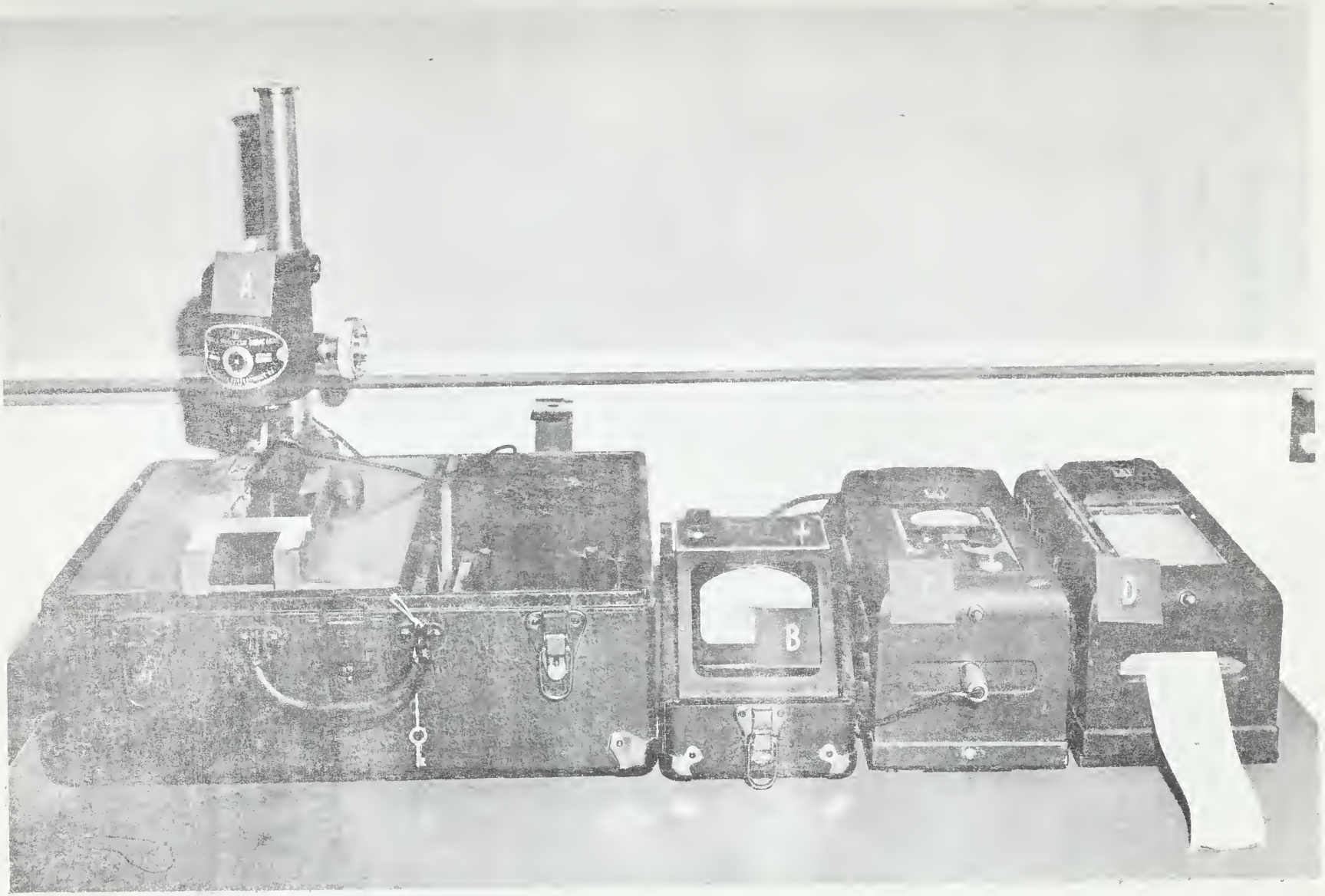

FIGURE 15 Surface Analyzer Equipment

FIGURE 15

EQUIPMENT IDENTIFICATION SYMBOLS

A Drive Head

B Averaging Meter

C Amplifier

D Oscillograph

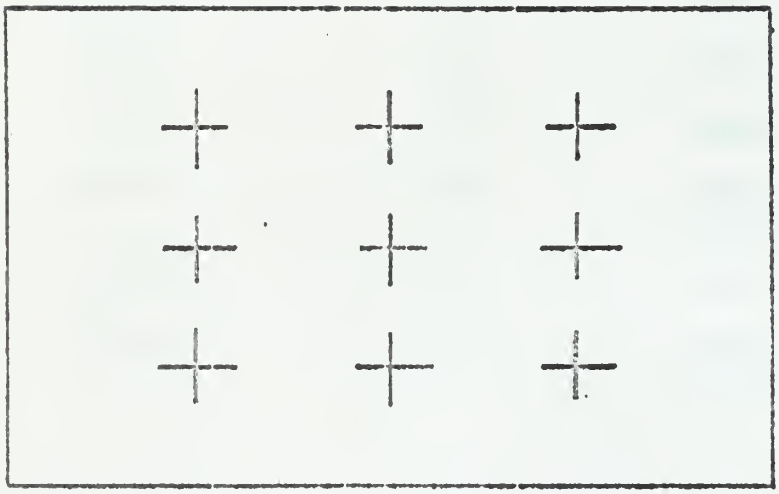

LOCATION OF SURFACE ROUGHNESS MEASUREMENTS

FIGURE 16

TABLE I

SPECIMEN IDENTIFICATION

NUMBER	ROUGHNESS (MICRO INCHES RMS)[1] BRUSH ANALYZER	VISUAL	PREPARATION
1	0.008"	--	shaped and milled
2	0.005"	--	shaped and milled
3	84-109	100	shaped and milled
4	40-52	50	shaped and milled
5	28-37	30	shaped
6	22-24	20	shaped and polished
7	13-17	16	shaped and polished
8	6.6-8.2	10	shaped, ground, lapped and polished
9	4.5-6.2	4	shaped and round
10	2.2-4.0	4	shaped, ground and polished

1 Roughness of specimens 1 and 2 are given in depth of cut on milling machine or shaper as appropriate.

TABLE II

SAMPLE DATA SHEET

Run No. 7

Date 14 Feb. 1962

Specimen No. 3

Time: Start 1030 Finish 2200

Thermocouple No.	1	3	4	6
Mv	6.21	6.29	6.30	6.19
°F	243.3	245.7	246.0	242.7
Mv	6.08	6.10	6.16	6.04
°F	239.0	239.7	241.7	237.7
Mv	5.96	5.96	6.02	5.90
°F	235.0	235.0	237.0	233.0
Mv	5.80	5.79	5.85	5.73
°F	229.7	229.3	230.3	227.3
Mv	5.64	5.62	5.66	5.58
°F	224.3	223.7	225.0	222.3
Mv	5.48	5.45	5.45	5.42
°F	219.0	218.0	218.0	217.0

Sheet 1 of 3

Thermocouple No.	2	5	7	8	9	10
Mv	8.19	8.02	5.10	5.15	5.10	5.12
°F	308.0	302.5	206.3	208.0	206.3	207.0
Mv	7.58	7.46	5.08	5.11	5.08	5.10
°F	288.0	284.3	205.7	206.7	205.7	206.3
Mv	7.11	7.04	5.06	5.09	5.06	5.07
°F	272.7	270.3	205.0	206.0	205.0	205.3
Mv	6.55	6.50	5.03	5.07	5.03	5.03
°F	254.3	252.7	204.0	205.3	204.0	204.0
Mv	6.09	6.05	5.00	5.04	5.00	5.00
°F	239.3	238.0	203.0	204.3	203.0	203.0
Mv	5.68	5.68	N O T N E E D E D			
°F	225.7	225.7				

WATER TEMP. °F	VOLT	AMPS
212.0	122.0	6.40
211.5	109.0	5.75
211.5	97.5	5.15
211.0	82.0	4.40
210.5	67.5	3.55
210.0	52.0	2.70